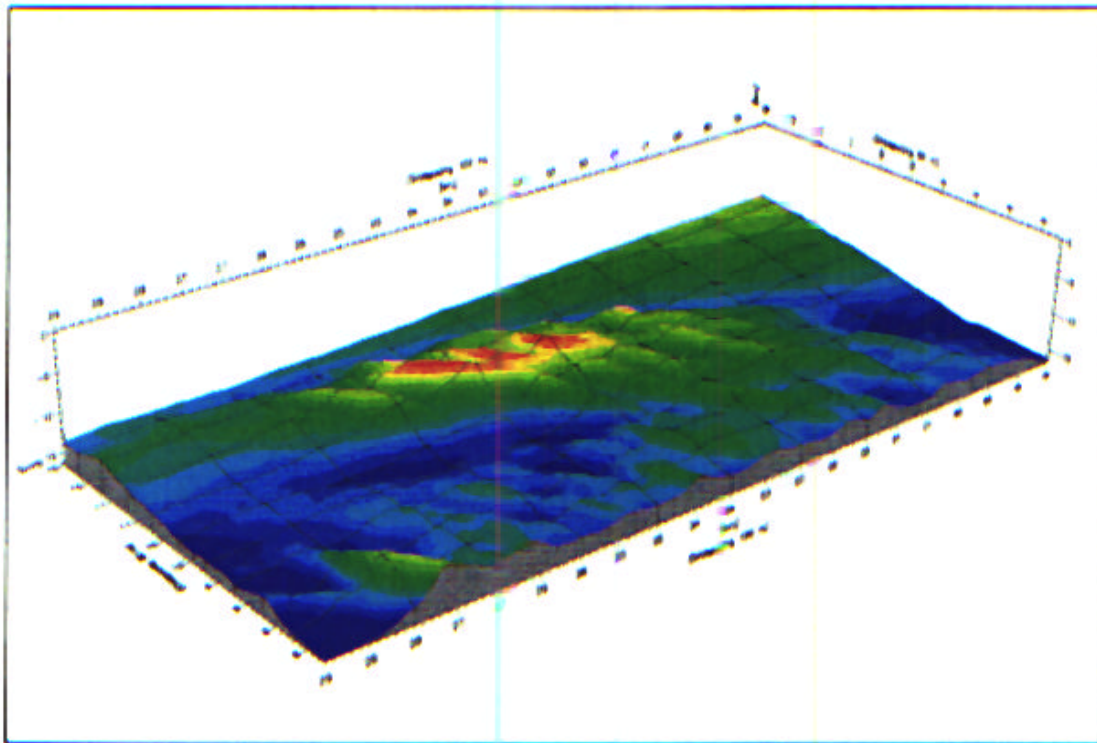


FINAL REPORT

A METHODOLOGY AND CRITERIA TO ASSESS THE IMPACT OF SAND VOLUME REMOVED IN FEDERAL WATERS ON THE NEARSHORE WAVE CLIMATE



PREPARED UNDER CONTRACT NUMBER
1435-01-97-00-14068

COASTAL ENGINEERING CENTRE
OLD DOMINION UNIVERSITY

AND

OLD DOMINION UNIVERSITY RESEARCH FOUNDATION



OCTOBER 1999

**A Methodology and Criteria to Assess the Impact of Sand Volume
Removed in Federal Waters
on the Nearshore Wave Climate**

for
Minerals Management Service
U.S. Department of Interior
Office of International Activities and Marine Minerals
381 Elden Street
Herndon, Virginia 22070-4817
(MMS #1435-01-97-00-14068)
Attention: Mr. Barry Drucker

by
Coastal Engineering Centre
Old Dominion University
Norfolk, Virginia 23529-0241
David R. Basco, Ph.D., P.E.

and
Old Dominion University Research Foundation
P.O. Box 6369
Norfolk, Virginia 23508-0369

Executive Summary

The Minerals Management Service (MMS) needs environmental information to make lease decisions at sand borrow sites used for beach nourishment. Long-term dredging from shoals and sand deposits has the potential for negative impacts to the nearshore wave climate.

This study employed the wave spectrum propagation model MIKE21.NSW (Danish Hydraulic Institute) to calculate wave transformations landward of the Sandbridge Shoal, sand borrow site in the Atlantic Ocean near Virginia Beach, Virginia as the test case. A clearly defined and rational methodology has been developed to quantify the change in wave climate (energy) before and after long-term sand dredging at the borrow site. The methodology defines the wave climate and how it is employed to determine the location of a reference line landward of the borrow site. Less than one percent of waves break seaward of the line so that linear, wave transformation processes can be modeled by a unit wave height at the offshore model boundary. The wave climate is then condensed to about 50 direction/period band combinations and wave height multiplier coefficients determined along the reference line for each combination. The weighted, total wave energy variation along the reference is then calculated for before and after sand is dredged to meet the long-term volume requirement of the borrow site. The percent change in total wave energy can then be found along the reference line as well as change in wave direction. This methodology is a rigorous, defensible way to quantify wave climate change.

We then employ the statistical theory of the null-hypothesis to test the significance of the difference of two medians in wave energy at the 95 percent confidence level for various locations along the reference line which is always long enough so that zero difference exists at both ends. Some positions along the reference line are acceptable and some are rejected by the null-hypothesis meaning the wave climate median energy has been significantly altered by the borrow site at that position. When more than 50 percent of the total reference line length is negatively impacted, we suggest that the borrow site, or the total volume of sand removal, and/or the dredging plan be rejected. Modifications can then be implemented and the process repeated to meet the MMS management criteria.

The above methodology and criteria has been labeled the Decision Tool Algorithm (DTA) for routine calculation by computer. The DTA is the final product of this research effort

and can be used to help the MMS determine which sites (if any) have potential negative impacts. Applied to the Sandbridge Shoal and 50-year, sand volume needs of the borrow site, we have concluded that the wave climate, will be negatively impacted. At this site and wave climate wherever the wave energy change exceeded 3-4 percent, the null-hypothesis was rejected so that about 63 percent of the reference line was negatively impacted. We recommend that the sand volume removed and/or dredge plan (area, depth, etc.) be modified and re-analyzed by this method to determine that which meets the MMS management criteria.

Other sites and wave climates may not correlate rejection and wave energy change percentage at the 3-4 percent level so that this result for Sandbridge Shoal should also be viewed with caution. Further research is required at other sites. We also recommend further research to incorporate changes in wave direction in the decision algorithm.

Table of Contents

Executive Summary	í
Table of Contents	ii
List of Figures	v
List of Tables	viii
Acknowledgment	ix
1.0 Introduction	1
2.0 Literature Review	3
3.0 Theory and Numerical Models	9
3.1 Open Coastal Area Wave Modeling	9
3.2 Parametric, Spectral Model	11
3.3 Review of Theory of Parametric Model	12
3.4 The MIKE21.NSW Model	14
3.5 Calibration and Applications	20
4.0 Quantifying Wave Climate Change-Test Case	21
4.1 Basic Questions	21
4.2 Sandbridge Shoal	21
4.3 Wave Climate Specification	22
4.4 Wave Model Calibrations	24
4.5 Wave Climate Change	31
4.6 Wave Energy Variability	34
4.7 Sandbridge Shoal Borrow Site	39
4.8 Wave Energy Change	48
5.0 Decision Tool for Management	56
5.1 The Null-Hypothesis Theory	56
5.2 Application to Sandbridge Shoal	58
5.3 The Decision Tool Algorithm (DTA)	60
6.0 Generic Studies With Idealized Bathymetry	61

7.0	Summary	62
7.1	Conclusions	62
7.2	Recommendations	64
	References Cited	65
	Appendices	
	A - WHEREWAVE Results	68
	B - Source Codes	72

Acknowledgments

The work performed herein was under Minerals Management Service contract #1435-01-97-00-14068 between March 1997 and May 1999. Contracting officer was Sandra L. McLaughlin and Dr. Barry S. Drucker, Environmental Studies Coordinator, was the technical monitor.

We wish to thank Dr. Jerome P.-Y. Maa and Mr. Woody Hobbs of the Virginia Institute of Marine Science (VIMS) for providing bathymetric data of the Sandbridge Shoal and also Dr. John D. Boon, VIMS for an early copy of his report on nearshore waves and currents at the study site.

The author also wishes to acknowledge the contributions of Murat Utku, Frank Lonza and Takashi Okomoto, graduate students in coastal engineering at Old Dominion University who all worked on this project at various times. Contract monitor for the Old Dominion University Research Foundation was Jackie Royster.

Errors and omissions are the sole responsibility of the author.

**Criteria to Assess the Impact of Sand Volume
Removed in Federal Waters
on the Nearshore Wave Climate**

1.0 Introduction

The search for suitable sand resources for beach nourishment projects has moved offshore into Federal government waters. The Minerals Management Service (MMS) of the Department of Interior needs environmental assessment criteria to make lease decisions. Long-term dredging with significant sand removal from shoals and sand deposits in federal waters has the potential for negative impacts to the nearshore, water wave climate (Fig.1).

Numerical models are useful for assessment of water wave modifications as waves travel over the areas dredged by sand mining activities. Under the National Environmental Policy Act (NEPA) the MMS is only required to assess the impacts to the *waves* resulting from the mining activities. This study employed the wave spectrum propagation model MIKE 21.NSW (Danish Hydraulic Institute, DHI) to determine wave climate change landward of the Sandbridge shoal, sand borrow area off the Southeastern Virginia coast as a test case. The main objective was the development of assessment criteria and the hypothesis for acceptance or rejection to quantitatively determine which sand borrow sites (if any) have potential negative impacts.

Section 2 briefly reviews the available literature. A summary of open coast wave models and details regarding the MIKE 21. NSW model are presented in Section 3. Then, in Section 4, we have asked a series of key questions regarding how to quantify wave climate change. The Sandbridge Shoal as a test case is then examined in detail in Section 4 including our answers to these questions. We then develop a standard, quantifiable, and statistically defensible method labeled the Decision Tool Algorithm (DTA) in Section 5. The DTA is the product of this research effort and can be used to help determine which sites (if any) have potential negative impacts at the 95% confidence level.

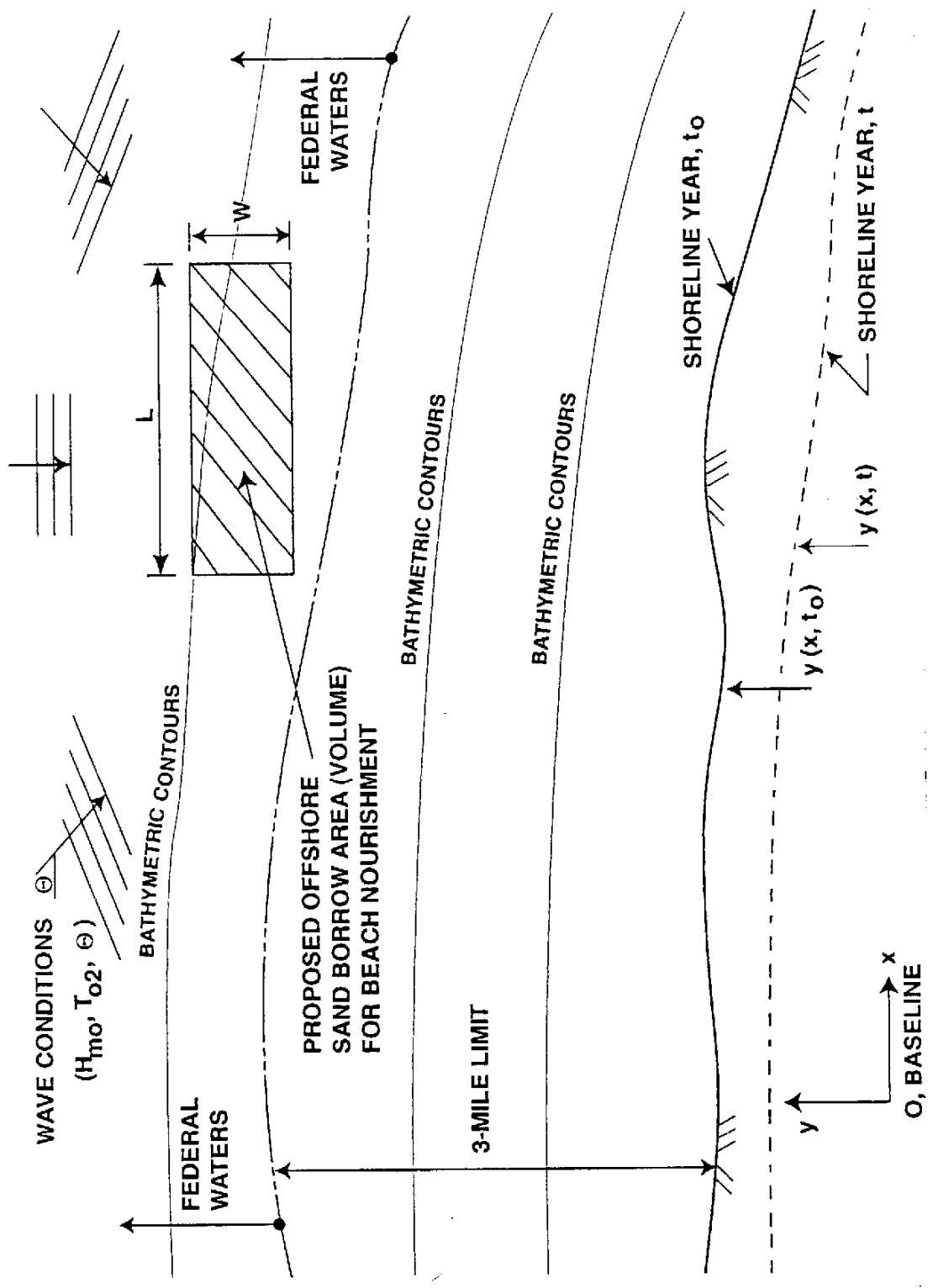


Figure 1 Definition Sketch (Plan View)

2.0 Literature Review

Theoretically, deeper water nearshore (submarine canyon, hole, bathymetry) spreads and hence reduces wave energy in the lee area landward of the depression. As shown in Fig. 2(b) (from Shore Protection Manual, 1984, Fig. 2-25, p. 2-73) wave rays are further apart directly landward, nearshore but also closer together in the adjacent, side regions. The canyon or hole focuses (increases) wave energy in both side areas.

Fig. 2(a) shows the exact opposite trend of a submarine ridge (shoal, mound, bathymetry, etc) causing wave focusing in the lee area. The wave tank experiments of Berkhoff, Booij and Radder (1982) employed an elliptical shoal superimposed on a plane beach. The shoal acts as a lens and focuses incoming wave energy into a strong convergence zone. These physical experiments are often employed to test numerical wave transformation models (see, e.g. Ebersole, et al., 1986 for tests of the RCPWAVE model of the Corps of Engineers). Fig. 3 displays the elliptical shoal case and some numerical model and observed data results for cross-section 3 behind the shoal. Removal of offshore shoals has the potential for significant modification of the leeward wave conditions.

Motyka and Willis (1974) studied wave refraction changes and resulting longshore sediment transport and shoreline change in a numerical model of a dredged area (hole) about 880m long, 305m wide and 4m deep in 7m water depth about 500m offshore. A schematic diagram of the expected changes in wave height is sketched in Fig. 4 to produce the effects on the original shoreline showing erosion and accretion areas as in Fig 5 (from Motyka and Willis, 1974). Deeper water nearshore produces larger breaking waves nearshore and gradients in sediment transport with a nodal zone causing sediment to move away in both directions from the erosion area. These littoral drift and geometric changes of the shoreline produced by nearshore, dredged holes are beyond the scope of this study. The erosional embayment and adjacent Accretional cusps that developed on the shoreline of Grand Isle, Louisiana in response to offshore dredging appear to correspond to that obtained in the numerical model of Fig. 5 (Combe and Soileau, 1987).

The Corps of Engineers employed the monochromatic version of the numerical model REF/DIF (Dalrymple and Kirby, 1991) to study nearshore wave change by sand mining offshore shoals near Ocean City, Maryland (Corps of Engineers, 1996). They introduced a nearshore

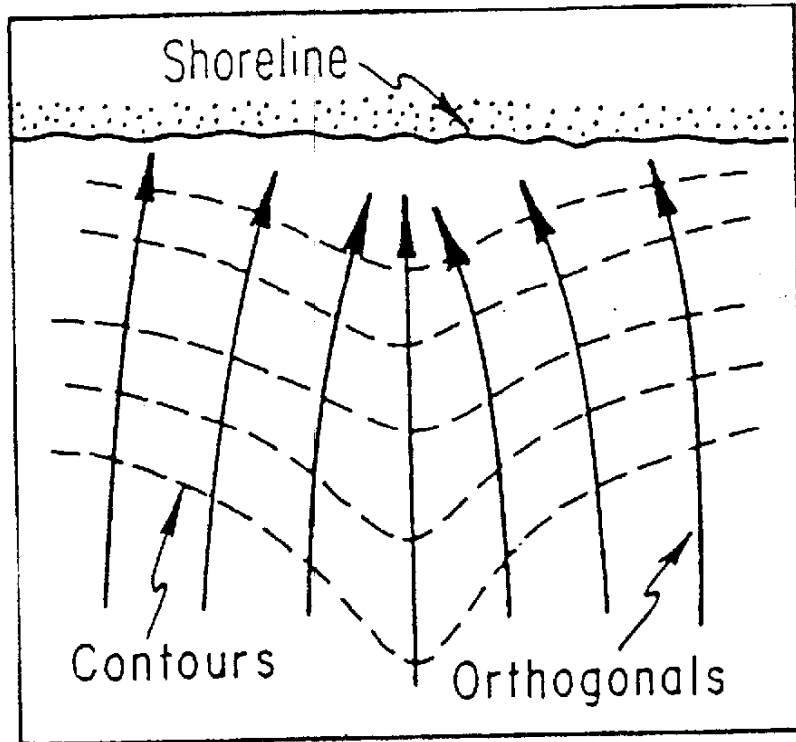


Fig. 2(a) Schematic of wave focusing in lee of shoal, ridge or mound

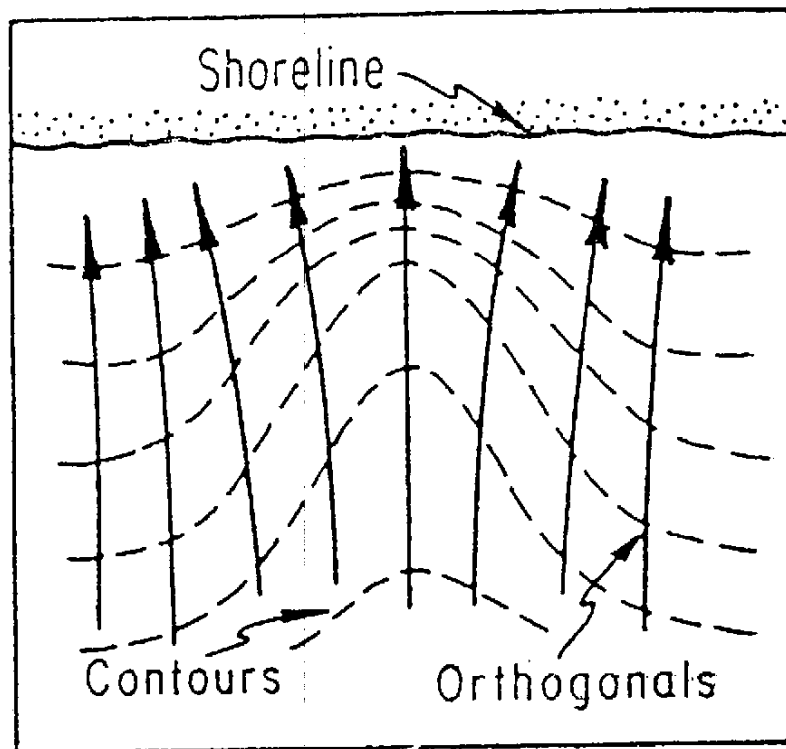
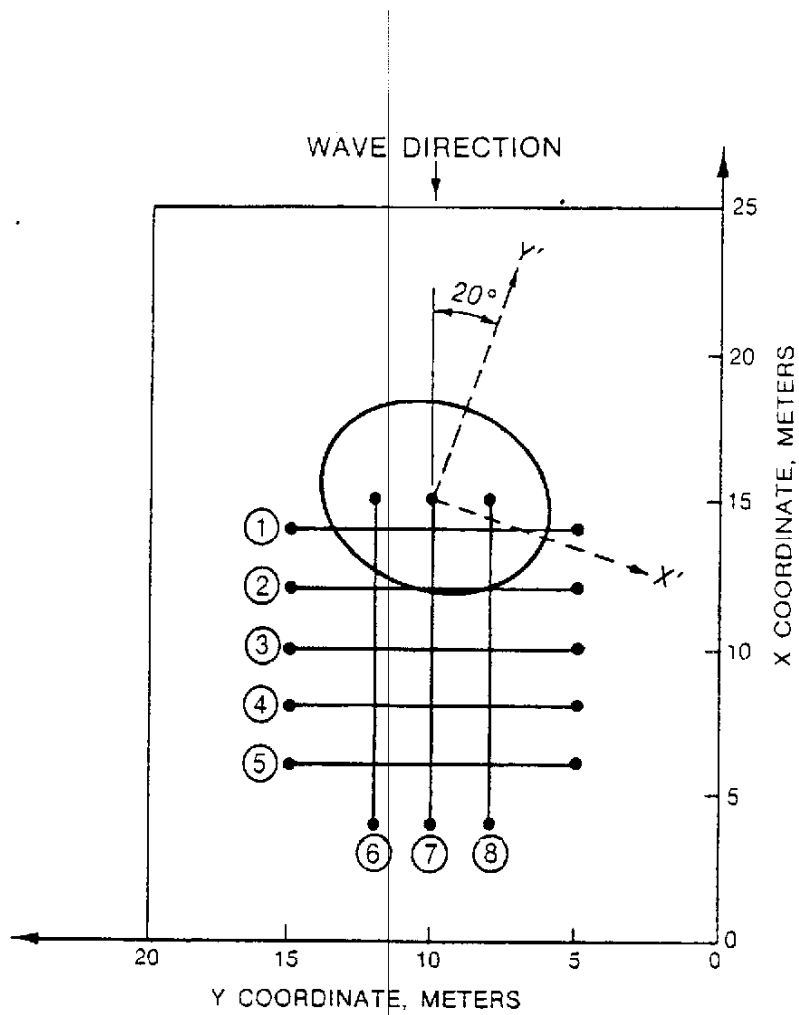


Fig. 2(b) Schematic of wave spreading in lee of submarine canyon, hole or depression



Geometry used in the model simulation of the elliptical shoal case

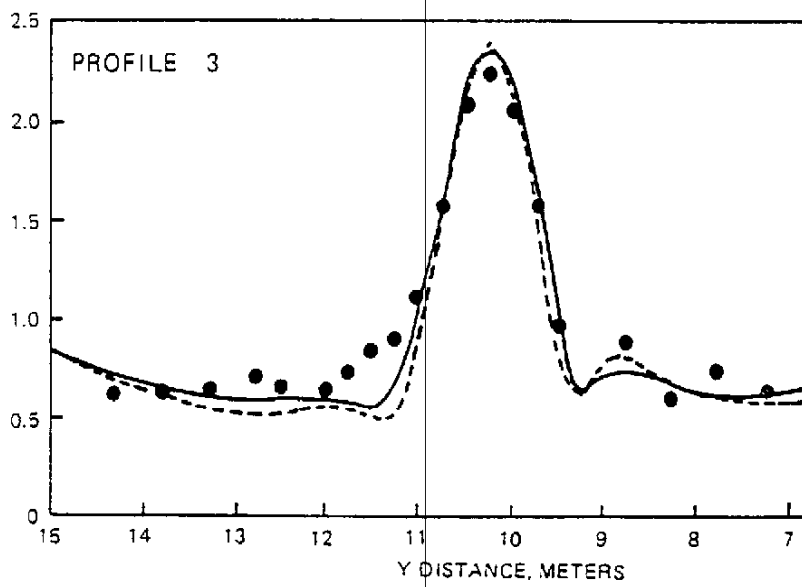


Fig. 3 Elliptical shoal and results of model and measured data (from Ebersole, et al., 1986)

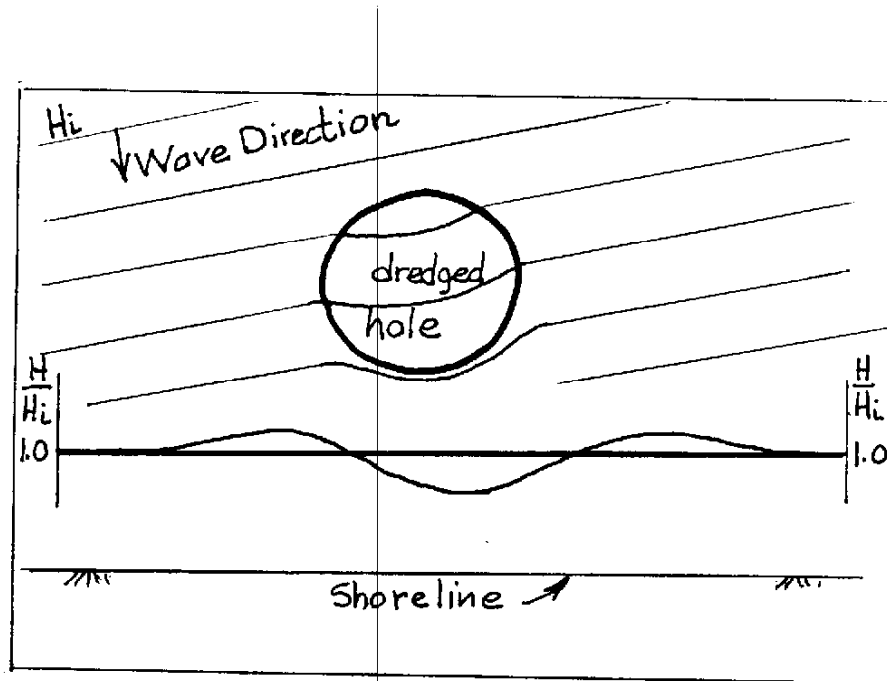


Fig. 4 Schematic diagram of expected changes in wave height due to nearshore dredging.

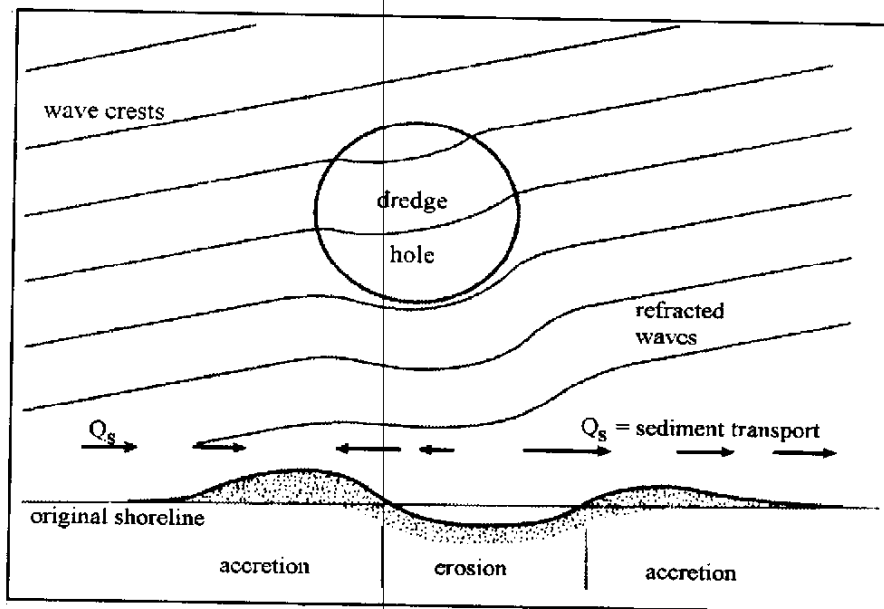


Fig. 5 Schematic of expected changes on original shoreline showing erosion and accretion area (from Motyka and Willis, 1974)

reference line and employed a unit wave height (1.0m) along the offshore boundary to study wave height (multiplier) change along the reference line. Fig. 6(a) is an example for one wave period and direction showing both wave height and direction variation along the reference line south of Ocean City Inlet. Then, after shoal removal by dredging, Fig. 6(b) displays wave height change and direction change along the reference line. Note that both the height and direction changes return to zero at both ends of the reference line. However, this study did not consider all waves present in a wave climate and did not attempt to define criteria to quantitatively assess the magnitude of the relative change found in the modeled results.

Maa and Hobbs (1998) studied the impact of dredging the Sandbridge Shoal off the coast of Southeastern Virginia on the wave patterns and resulting sediment transport along the coast. The numerical model RCPWAVE (Ebersole, 1985) for monochromatic waves was employed to investigate breaking wave height change and breaking angle change after dredging. It was concluded that the modified shoal produced "insignificant" physical impact on the adjacent coast but the criteria to make this judgement was not defined. Wave ray convergence in the leeward zone of the shoal for long period waves coming from the NE was found to diminish after dredging the shoal. The historic, natural, severe erosion rate at Sandbridge (-3m/yr) was suggested to possibly be related to a wave energy convergence zone leeward of the Sandbridge Shoal.

Boon and Hobbs (1998) also studied changes in wave conditions after sand removal from the Sandbridge Shoal near the City of Virginia Beach, Virginia. They employed the spectral version REF/DIF, S (Kirby and Azkan, 1992) to qualitatively display color maps of wave heights before and after dredging one area of the Sandbridge Shoal to -3m. Only three extreme wave conditions were considered ($H_{mo} = 4$ to 7 m, $T_p = 12$ to 15 s) and the effect of dredging was again found to decrease the spectral significant wave height (about 0.5 m max) in the down-wave, shadow-zone approaching the surf zone. No information was provided on wave direction.

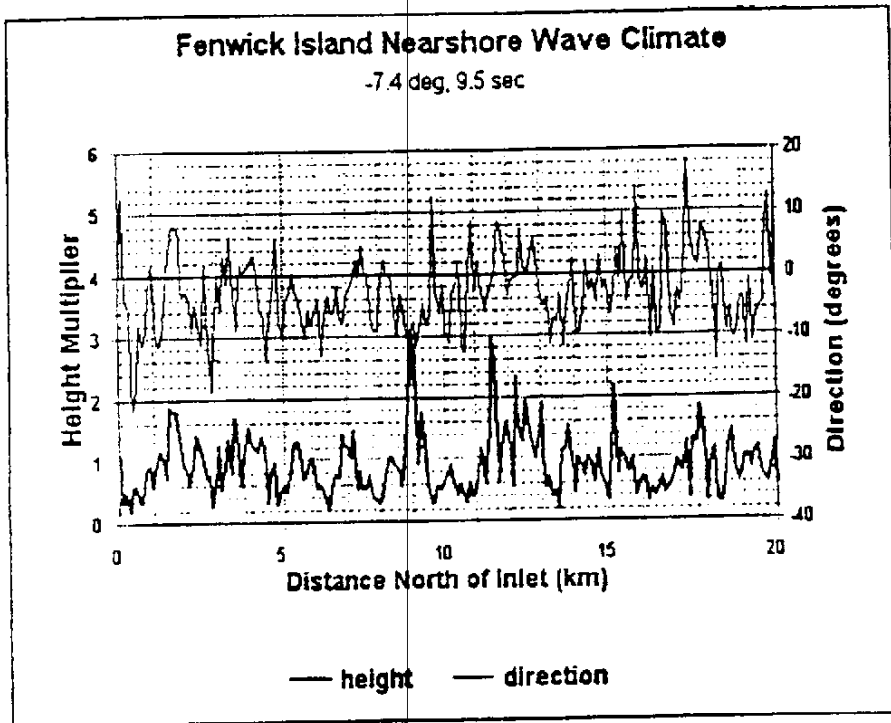


Fig. 6(a) Example of unit wave height and direction variability along reference line for one wave direction and period (from Corps of Engineers, 1996)

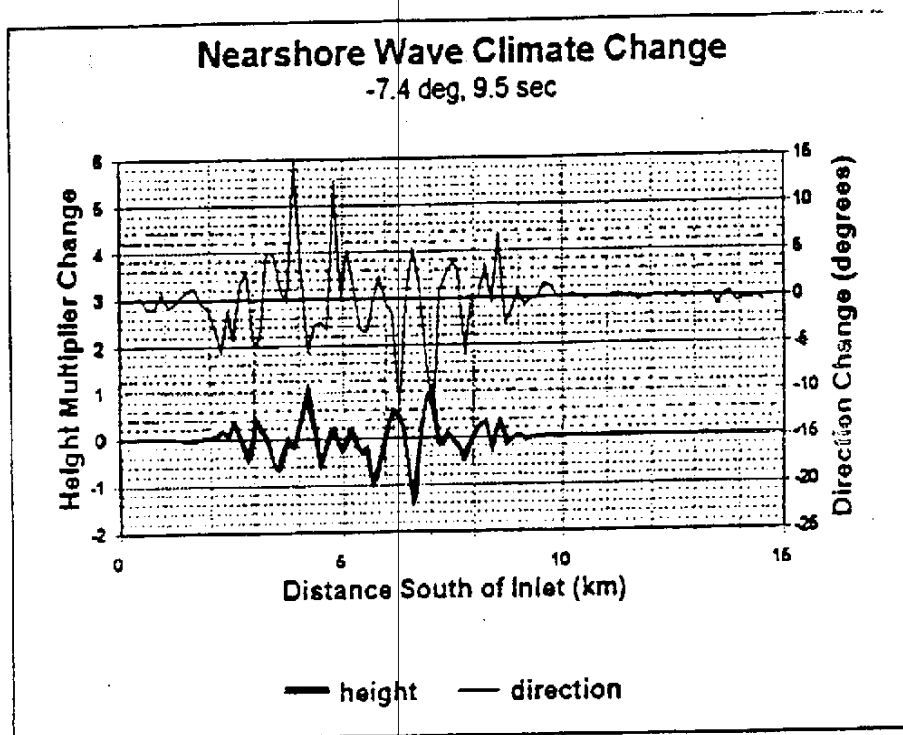


Fig. 6(b) Wave height and direction change along the reference line for same conditions in Fig. 6(a) but after sand volume removed from borrow site.

3.0 Theory and Numerical Models


3.1 Open Coastal Area Wave Modeling

Various wave theories based on two fundamentally different concepts and approximations within each concept are available for modeling waves in the open coastal environment. Fig. 7 displays six wave modeling systems available in the class called MIKE21 as developed by the Danish Hydraulic Institute, Horsholm, Denmark. Three are based on the conservation of wave energy (or action density) concept including classic wave ray tracing methods. A second three are rooted in the conservation of momentum (and mass) that permit wave phase relationships to be resolved in the model. All energy-based wave models are phase-averaged. The vertical column lists features that are included in the underlying physics of the theory and/or added empirically (e.g. breaking) in most numerical models. Each model has certain strengths and weaknesses for particular applications.

The RCPWAVE and REF/DIF models cited above are parabolic wave models based on the mild slope equation of Berkhoff (1972). Because wave diffraction effects are included, these models can be used to estimate wave energy spreading behind coastal structures (breakwaters, jetties, etc.) and coastal islands, headlands, etc. However, in open coastal areas, wave diffraction is not significant (see, e.g. Komen, et al., 1994). In some cases, (e.g. the Boussinesy model) the computing facilities and expense of running the "complete" models are well beyond the accuracy and economic resources available for the intended application.

Fully discrete, spectral models based upon energy concepts require maximum space and speed available on digital computers. The directional wave spectrum at each computation node includes 10-15 discrete spectral (frequency) components. This full computational effort may not be warranted for this application. The fully discrete spectral model (SHALWV) is available from the Coastal Engineering Research Center (CERC) of the Army, Corps of Engineers.

Recently, the fully discrete, spectral model (SWAN) as developed in the Netherlands (Booij, Holthuijsen and Ris, 1996) has been identified as a "community model" by the Office of Naval Research (ONR) and is now available over the Internet (Holtuijsen, 1997). The Waves in Shallow Water Environments (WISE) group has annual meetings dedicated to discussions of the physics, coupling, numeric's, measurements and all aspects of wave modeling in shallow water. The most

	ENERGY/WAVE ACTION CONCEPT			MOMENTUM CONCEPT		
	FULLY DISCRETE SPECTRAL MODEL	PARAMETRIC/DISCRETE SPECTRAL MODEL	RAY MODEL	MILD SLOPE PARABOLIC	MILD SLOPE ELLIPTIC	BOUSSINESQ
	MIKE 21 OSW	MIKE 21 NSW	REFRACTION MODEL	MIKE 21 PMS	MIKE 21 EMS	MIKE 21 BW
TIME VARYING	●					●
DIRECTIONAL SPREADING	●	●		●		●
FREQUENCY SPREADING	●			●		●
SHOALING	●	●	●	●	●	●
REFRACTION	●	●	●	●	●	●
DIFFRACTION				○	●	●
REFLECTION & BACK SCATTER	○				●	●
BOTTOM FRICTION	●	●	●	●	●	●
BREAKING	○	●	●	●	●	
WIND GENERATION	●	●				
NON-LINEAR WAVE						●
WAVE-WAVE INTERACTION	○					●
WAVE-CURRENT INTERACTION		●				
WAVE-SHIP INTERACTION						●

● INCLUDED

○ PARTLY INCLUDED

Fig. 7 Wave modeling systems available at the Danish Hydraulic Institute, Horsholm, Denmark

recent meeting in Annapolis, MD (March, 1999) included many papers on the SWAN model. At this writing, it is not clear whether or not the ability to fully model the spectral shape at each computational mode is warranted for this application. The writer is not aware of any studies directly comparing the fully discrete and parametric discrete spectral models under identical conditions in the open coastal ocean. Relatively small increases in the bottom depths over large areas as performed by hydraulic dredges for sand mining should have little or no major impact on the spectral shape. For this reason, we believe that the parametric, discrete spectral model is best suited for this application.

3.2 Parametric, Spectral Model

Parameterization of the spectral shape while retaining the directional spreading reduces the computational effort. A parametric, spectral, numerical model for the hindcasting of waves in shallow-water was first developed by Holthuijsen, Booij and Herbers (1989) at Delft University of Technology, the Netherlands and was the forerunner of the SWAN model. The model is based on an Eulerian presentation of the spectral action balance of the waves propagating across a grid rather than the Lagrangian presentation along wave rays. The model accounts for refractive propagation of short-crested waves (seas) over arbitrary bottom topography and across current fields. The effects of wave growth and dissipation due to wind generation, bottom dissipation and wave breaking (both deep and shallow water) are represented as source terms in the action balance equation. Computational efficiency is enhanced by removal of time as an independent variable to obtain a steady state model. This is justified by the relatively short travel time of waves in coastal regions.

A second simplification is the parameterization of the basic balance equation in terms of mean frequency and a frequency-integrated action density, both functions of the spectral wave directions. The complete spectral representation of wave directionality is retained. The version of the model as developed at the Delft University is called HISWA (Holthuijsen, Booij and Herbers, 1989). The developers of both the parametric version (HISWA) and the full spectral model (SWAN) at Delft University have concluded that in terms of significant wave height HISWA and SWAN will not be very different for open ocean conditions (Holthuijsen and Booij, personal comm., 5/12/99).

The Danish Hydraulic Institute also produced a software package labeled the Nearshore

Spectral Wind-Wave module (MIKE21.NSW, 1991). With respect to the basic equations and description of the source terms, MIKE21.NSW is based on the approach proposed by Holthuijsen, Booij and Herbers (1989).

Both HISWA and MIKE21.NSW have been tested against analytic solutions and under laboratory conditions (Booij, 1985; Dingerans et al., 1986; Booij et al., 1988; Bondzie, 1992; Bondzie and Panchang, 1993) and against extensive field data sets (Holthuijsen, Booij and Herbers, 1989; Bondzie and Panchang, 1993; den Adel et al., 1990; Ris et al., 1994; and Trindade et al., 1993) from the Netherlands, Canada, Australia and the US. The USGS has conducted field verification of HISWA in Florida and Louisiana on Lake Ponchatrain (List, 1996).

3.3 Review of Theory

In the presence of an ambient current the relevant wave parameter for modeling purposes is action density A defined as (e.g. Whitham, 1965)

$$A(\omega, \theta, x, y, t) = E(\omega, \theta, x, y, t) / \sigma \quad (1)$$

with the intrinsic wave frequency, σ defined relative to coordinates moving with the local current velocity, \bar{U} . In Equation (1), E is the wave energy density typically modeled in an energy balance equation as a function of absolute frequency, ω and direction, θ and considered a slowly varying function in space (x, y) and time t . The absolute frequency, ω relative to fixed coordinates is

$$\omega = \sigma + \bar{k} \cdot \bar{U} \quad (2)$$

with \bar{k} , the wave number vector (magnitude k and direction θ). Equation (2) can be considered as the Doppler equation since the second term on the right (dot product) produces a scalar that is equivalent to the Doppler shift. In an Eulerian reference frame, the action balance equation then becomes (here dropping the independent variable notation for A)

$$\frac{\partial A}{\partial t} + \frac{\partial}{\partial x}(C_x A) + \frac{\partial}{\partial y}(C_y A) + \frac{\partial}{\partial \theta}(C_\theta A) + \frac{\partial}{\partial \omega}(C_\omega A) = T \quad (3)$$

where the first term on the left side is the local rate of change of action density (for non-stationary problems) and the other terms on the left represent net transport of action density in space (x, y),

direction θ , and absolute frequency ω domains, respectively. C denotes the propagation speed in the x, y, θ and ω independent variables. The total effects of wave generation, interaction, dissipation and current blocking of action are all represented by the action source function, T . The source function terms are also a function of x, y, t, θ and ω .

In a typical application of the action balance equation for modeling (e.g. Tolman, 1988; 1991) first order Stokes linear wave theory is used to give the dispersion equation for the intrinsic frequency

$$\sigma^2 = gk \tanh(kd) \quad (4)$$

where k is the wave number, d is the water depth and the absolute group velocity, C_g for wave energy flux

$$\bar{C}_g = \frac{\partial \sigma}{\partial k} \frac{\bar{k}}{k} + \bar{U} \quad (5)$$

Here, the direction of the absolute group velocity, \bar{C}_g is altered by the current direction and in general not equal to the wave direction, θ (normal to the wave crest of wave component (θ, ω)). The space direction, propagation speeds (C_x, C_y) in Equation (3) are simply the x - and y - components of the action propagation speeds, i.e. the group velocity components (C_{gx}, C_{gy}) as given by Equation (5) relative to a fixed coordinate system (the subscript "g" is dropped for ease of notation).

The propagation speed C_θ in the directional domain is given by linear wave theory as

$$C_\theta = -\frac{1}{k} \frac{\partial \sigma}{\partial d} \frac{\partial d}{\partial n} - \frac{\bar{k}}{k} \cdot \frac{\partial \bar{U}}{\partial n} \quad (6)$$

where d is the local water depth and n is the coordinate in (x, y) space normal to the spectral wave direction θ . This term represents refraction including current effects since action density rather than energy density is used in the formulation.

The propagation speed C_ω represents the shift of action density in the frequency domain due to time variations in the propagation medium (variations in the water depth or current speed and direction). It is given by

$$C_{\omega} = \bar{k} \cdot \frac{\partial \sigma}{\partial d} \frac{\partial d}{\partial t} \quad (7)$$

For the HISWA (Holthuijsen et al., 1989) and MIKE 21 NSW (DHI, 1991) models, the wave field, the water depth and the current fields are considered as constant in time. In such a situation the first and the fifth term on the left-hand side of the action balance equation vanish.

A parameterization of the equation in the frequency domain is performed by introducing the zeroth and the first moment of the action spectrum as dependent variables. This lead to the following coupled partial differential equations

$$\frac{\partial}{\partial x}(C_{ox}m_o) + \frac{\partial}{\partial y}(C_{oy}m_o) + \frac{\partial}{\partial \theta}(C_{o\theta}m_o) = T_o \quad (8)$$

$$\frac{\partial}{\partial x}(C_{1x}m_1) + \frac{\partial}{\partial y}(C_{1y}m_1) + \frac{\partial}{\partial \theta}(C_{1\theta}m_1) = T_1 \quad (9)$$

and the moments of the action density spectrum are defined as

$$m_n(\theta) = \int_0^{\infty} \omega^n A(\omega, \theta) d\omega \quad (10)$$

where ω is the absolute frequency, A is the spectral action density and $n=0$ and 1 for the zeroth and the first moment of the action spectrum. C_{ox} , C_{oy} and $C_{o\theta}$ in Equation (8), and C_{1x} , C_{1y} and $C_{1\theta}$ in Equation (9) are the group velocities through (x, y, θ) -space of m_o and m_1 , respectively. The left hand side of the basic equations (Equation 8 and 9) takes into account the effect of refraction and shoaling. The source terms T_o and T_1 take into account the effect of local wind generation and energy dissipation due to bottom friction and wave breaking. The effects of currents on these phenomena are also included.

3.4 MIKE 21 NSW Model

The basic transport equations are solved using the finite difference method. The zeroth and first moment of the action spectrum are calculated on a rectangular grid (Fig. 8(a)) for a number of discrete directions, θ as a third "dimension" depicted in Fig. 8(b). A once-through marching procedure is applied for the predominant direction of wave propagation (Fig. 8).

Three types of boundary conditions can be applied: essential, symmetry and absorbing types.

The essential type are in the form of wave parameters: significant wave height, mean wave period, mean wave direction, standard deviation from mean direction, and directional spreading index. The directional spreading index, n defines the width (i.e. narrow or broad) of the directional distributional spreading function for narrow (index $n=2$) and broad (index $n=64$) directional spectrums using the standard cosine power function. The symmetry boundary condition involves the derivative normal to the boundary and both gradients for the zeroth and the first moment are set equal to zero. The absorbing boundary condition is that no energy enters the model area and energy propagates out of the model area without reflections propagating back into the model area.

Bottom energy dissipation is based on the conventional quadratic friction law to represent bottom shear stress. The dissipation expression for one single frequency (Dingemans, 1983) has been extended by Holthuijsen et al. (1989) to include directional distribution of wave energy and influence of currents. This extended formulation is used in MIKE 21 NSW. The friction coefficient can be specified directly or calculated using an empirical expression (Johnson, 1966; Swart, 1974) using a Nikuradse roughness parameter. In both cases, values can be constant or as two-dimensional maps to vary the bottom roughness over the model area.

Wave breaking is formulated for large wave steepness (deep water) and limiting water depth (shallow water) and based on the formulation of Battjes and Janssen (1978). The effect of wave breaking on the mean wave period can also be included. Here, the assumption is that the dissipation of energy in breaking waves is concentrated on the low frequency side of the frequency spectrum. Hence, the wave breaking has the effect of lowering the mean wave period. Current effects on wave breaking is included in the source terms.

Finally, in MIKE 21 NSW the source terms for the local wind generation are derived directly from the Corps of Engineers, Shore Protection Manual (1984) formulation for fetch-limited, wave-growth in deep water. A stationary spatially uniform wind starts to blow over deep water (no currents, no waves) at time $t = 0$. Wind speed and direction can also be specified as a two-dimensional map over the model area.

In this application, if the ambient current field is assumed zero, the fundamental, action balance equation reduces to the energy balance for total wave energy density, E . The basic output

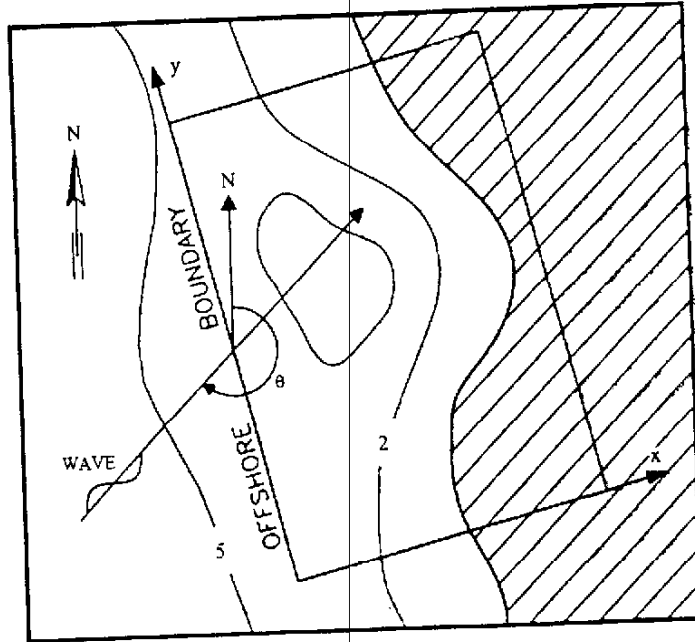


Fig. 8(a) Rectangular grid in MIKE21.NSW model

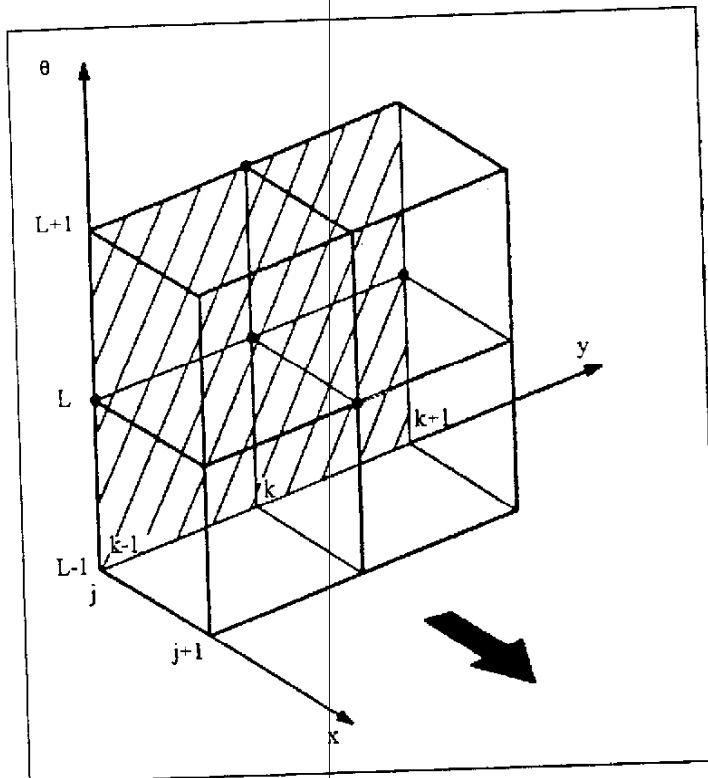


Fig. 8(b) Grid cell showing discrete directions, θ as third "dimension".

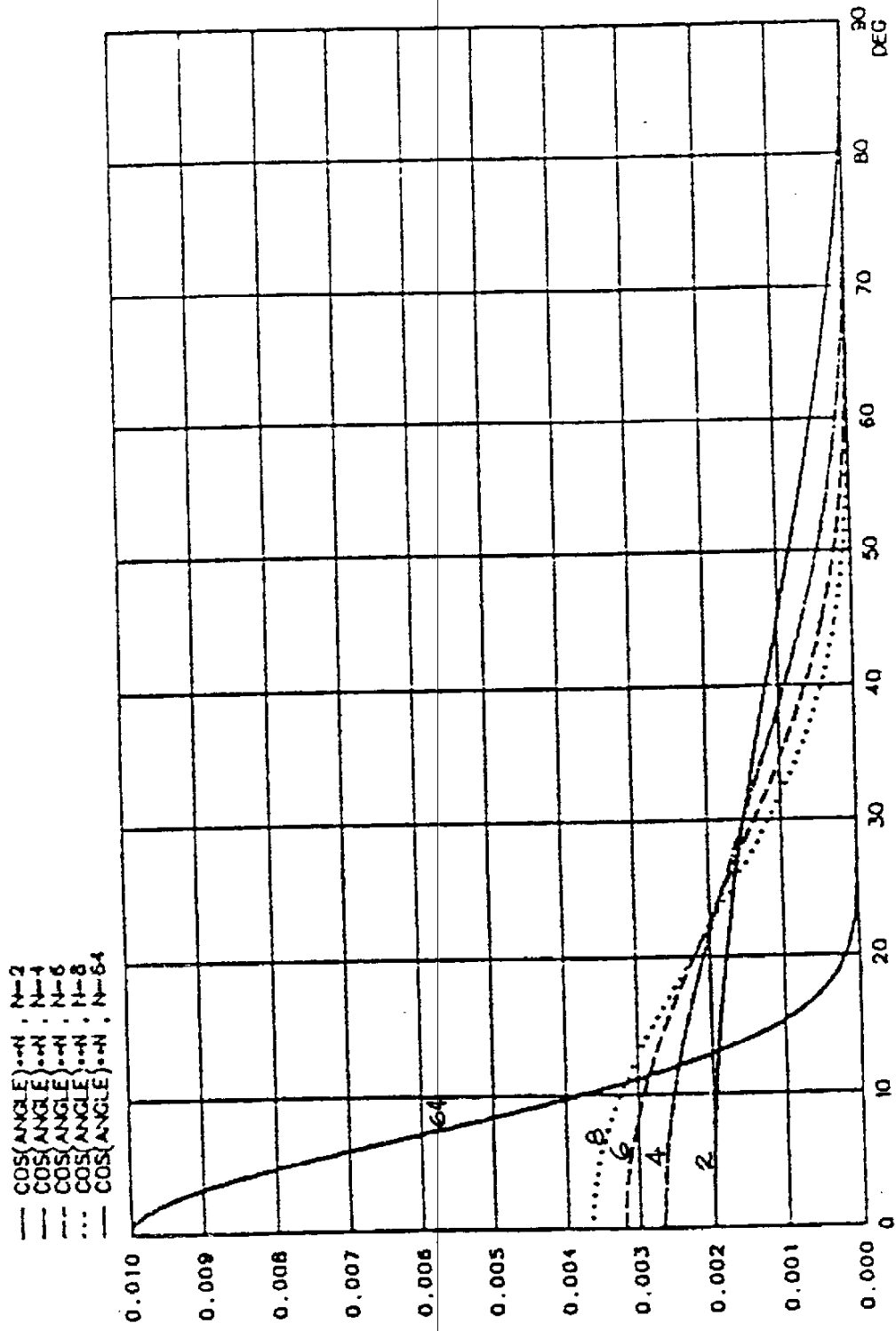


Fig. 9 Directional spreading function for range of directional spreading shapes.

products from MIKE 21 NSW consist of two-dimensional arrays containing the following integral wave parameters. The spectrally significant wave height, H_{m0} is defined by

$$H_{m0} = 4\sqrt{E_0}, \quad E_0 = \int_0^{2\pi} E(\theta) d\theta \quad (11)$$

where E and E_0 are the wave energy density and total wave energy, respectively, and θ is the wave direction. The mean wave period, T_m is defined by

$$T_m = \frac{2\pi}{\omega_1} \quad (12)$$

where,

$$\omega_1 = \frac{\int_0^{2\pi} \int_0^{\infty} \omega E(\omega, \theta) d\omega d\theta}{\int_0^{2\pi} \int_0^{\infty} E(\omega, \theta) d\omega d\theta} \quad (13)$$

and ω is the absolute frequency. The mean wave direction, θ_m , and the directional standard deviation are also calculated. Results from MIKE 21 NSW can also be obtained in the form of two-dimensional arrays containing the x- and y- components of a vector showing mean wave direction in the model area.

In summary, the model propagates irregular, directional, spectral wave action density over arbitrary bathymetry across an x, y grid and each node contains the following integral wave parameters:

- spectral significant wave height, H_{m0}
- mean wave period, T_m
- mean wave direction, θ_m
- directional standard deviation; σ_r
- radiation stress components, S_{xx} , S_{yy} and S_{xy} .

Gradients in the radiation stress field drive the longshore currents which in turn cause sediment transports in the surf zone. But this area is beyond the scope of work for this study. Fig. 10 displays the menu structure for the MIKE 21 Nearshore Spectral Wind-Wave model.

Menu Structure

The following menus are used in the MIKE 21 Nearshore Spectral Wind-Wave module:

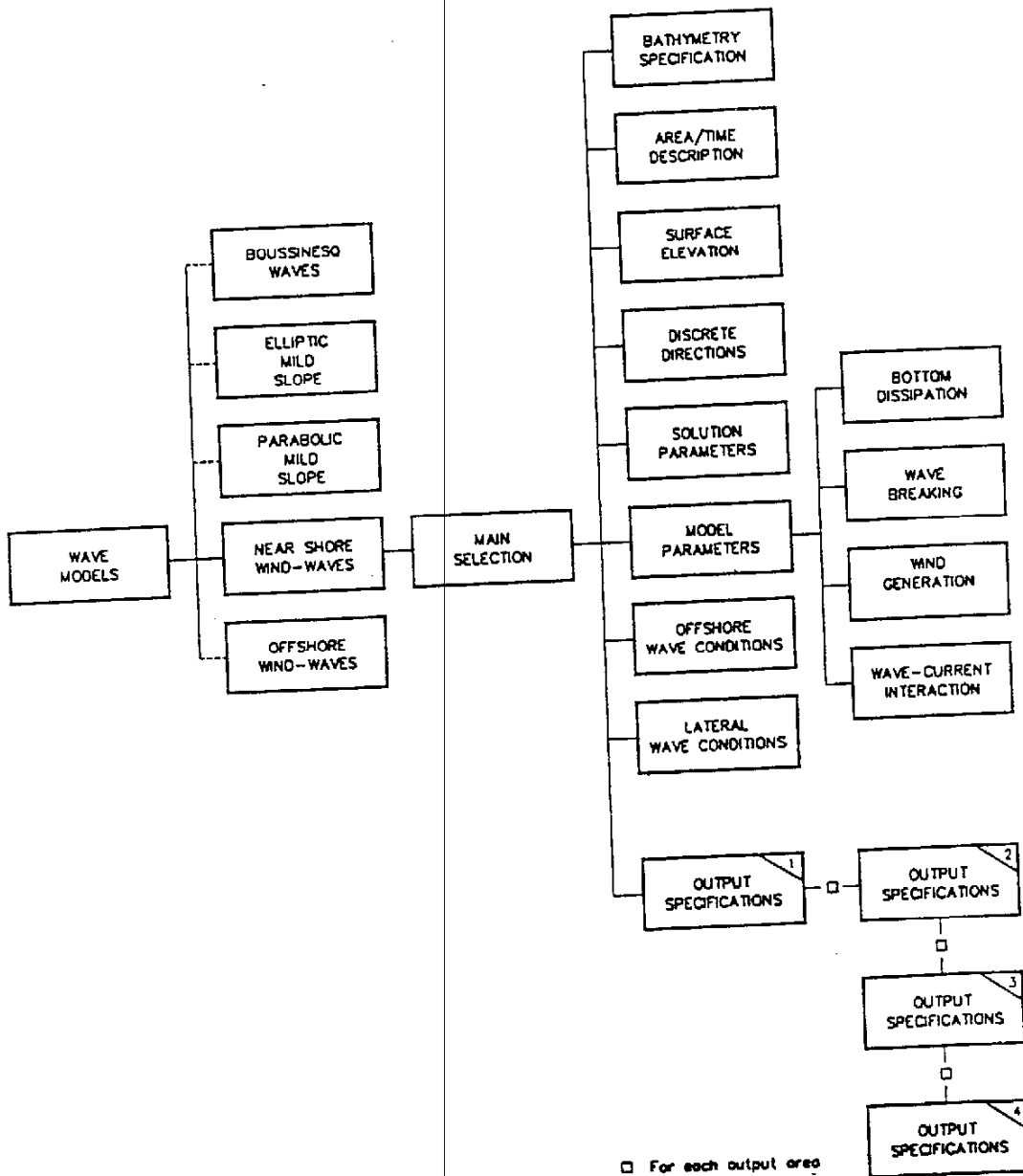


Fig. 10

Menu structure for MIKE21.NSW model

3.5 Calibration and Applications

Basco and Shin (1996) have calibrated the MIKE 21 NSW model against measured wave data at two locations within the Chesapeake Bay. Experience was obtained regarding the influence of grid size, directional spreading index, and bottom roughness on the wave heights for various storm conditions. This experience was helpful in the open ocean application discussed below.

The model has been applied under contract with Hayes, Seay, Mattern & Mattern, Inc., consulting engineers in Virginia Beach to develop wave design information for the Leeward Marina breakwater design in the James River. It has also been applied under contract with the Corps of Engineer, Norfolk District Office to develop design wave information for the Willoughby Bay shoreline at Monkey Bottom, Norfolk, VA.

The Coastal Engineering Center at Old Dominion University has a commercial license for application of MIKE 21 NSW since 1994. It is a menu driven, user friendly model that is designed to improve productivity of the user for multiple runs in a consulting engineering environment where final product accuracy, reliability and color, graphic display of the results is required. The new release; MIKE 21 Version 5.0 is 1999 will be a fully WINDOWS environment. The MIKE 21. NSW model is a useful tool for this application.

4.0 Quantifying Wave Climate Change-Test Case

4.1 Basic Questions

As discussed above in Section 2, a nearshore hole or removal of a shoal will spread wave energy in the lee area directly landward, and will focus wave energy in adjacent side areas. A large surface area can be influenced in the “shadow zone” landward of the sand mining site. In our research to assess the impact of sand volume removed on the nearshore wave climate we have asked the following questions:

1. How do you specify a wave climate? Do you use hindcast wave information (18-20 years) or measured wave data (variable time)?
2. How do you calibrate a wave model for wave climate?
3. Should you study wave change over the entire “shadow” area or along a meaningful reference line?
4. How do you locate a meaningful reference line (water depth)? How long do you make the reference line?
5. How can you condense the wave climate data set (height, period, direction, and number of events) to a practical number of numerical model tests to conduct?
6. How do you quantify the size and volume of sand removed over the design life? What is the design life (25 years, 50 years) of the borrow site? Is the volume removed from a shoal area or does it create a depression in the bathymetry?
7. How do you quantify wave climate change for both wave energy and wave direction.
8. Can you develop a standard, quantifiable and statistically defensible methodology to conclude that the dredging does (or does not) change the wave climate?

Our efforts to find answers to the above questions have been reported in Basco and Lonza, 1998, in the M.S. thesis of Lonza (1999) and herein below using as a test case, the Sandbridge Shoal, sand borrow area off the southeastern Virginia coast.

4.2 Sandbridge Shoal

The study area is the mid-Atlantic Ocean, coastal shelf region off southeastern Virginia

extending from the entrance to Chesapeake Bay at Cape Herry to the Virginia/North Carolina border (and south to Duck, NC) and offshore to the near edge of the continental shelf where NDBC Buoy 44014 is deployed as depicted in Fig. 11. This was the domain for a coarse grid wave model as discussed below.

Fig. 11 also shows the location of WIS Atlantic Hindcast Information; station WIS III 2058 of the Corps of Engineers (Brooks and Brandon, 1995) which was the boundary for the fine grid model. The Sandbridge Shoal borrow site location is also shown. Geophysical exploration in the late 1980's by the Virginia Institute of Marine Science (Kimball and Dame, 1989) revealed a moderately-sized sand shoal situated approximately three miles east of Sandbridge Beach. About 40 million cubic yards (cy) of clean, medium to coarse sand ($d_{50} = 0.34\text{mm}$) was found concentrated in a discrete shoal feature with no overburden. This shoal represents a valuable sand resource for beach nourishment as a borrow site because of its economical transport distance to Dam Neck beach, south of Rudee Inlet, Sandbridge beach, and the tourist beach for the City of Virginia Beach north of Rudee Inlet.

Additional vibracore boring data can be found in (Swean, 1998) for the Sandbridge Shoal borrow site. Further details and a three-dimensional, graphical representation of the shoal region bathymetry are found in Section 4.7.

4.3 Wave Climate Specification

The wave climate is the historical record of wave conditions: heights, periods, directions and number of events at a specified location. Measured wave data is available at three locations in Figure 11, namely (1) the deep water wave buoy NDBC 44014 at the edge of the shelf; (2) the wave gauges at the CERC, Field Research Faculty at Duck, North Carolina and (3) the directional, nearshore wave gauge VA001 located in 8m water depth due east of the 15th street pier in Virginia Beach (not shown). Some of this data has been employed in the coarse and fine grid model calibration discussed in the next section. However, in general, the length of record is less than that needed to specify a statistically valid wave climate. Non-directional wave data is also available at the entrance to the Chesapeake Bay (Lighttower CHLV 2)

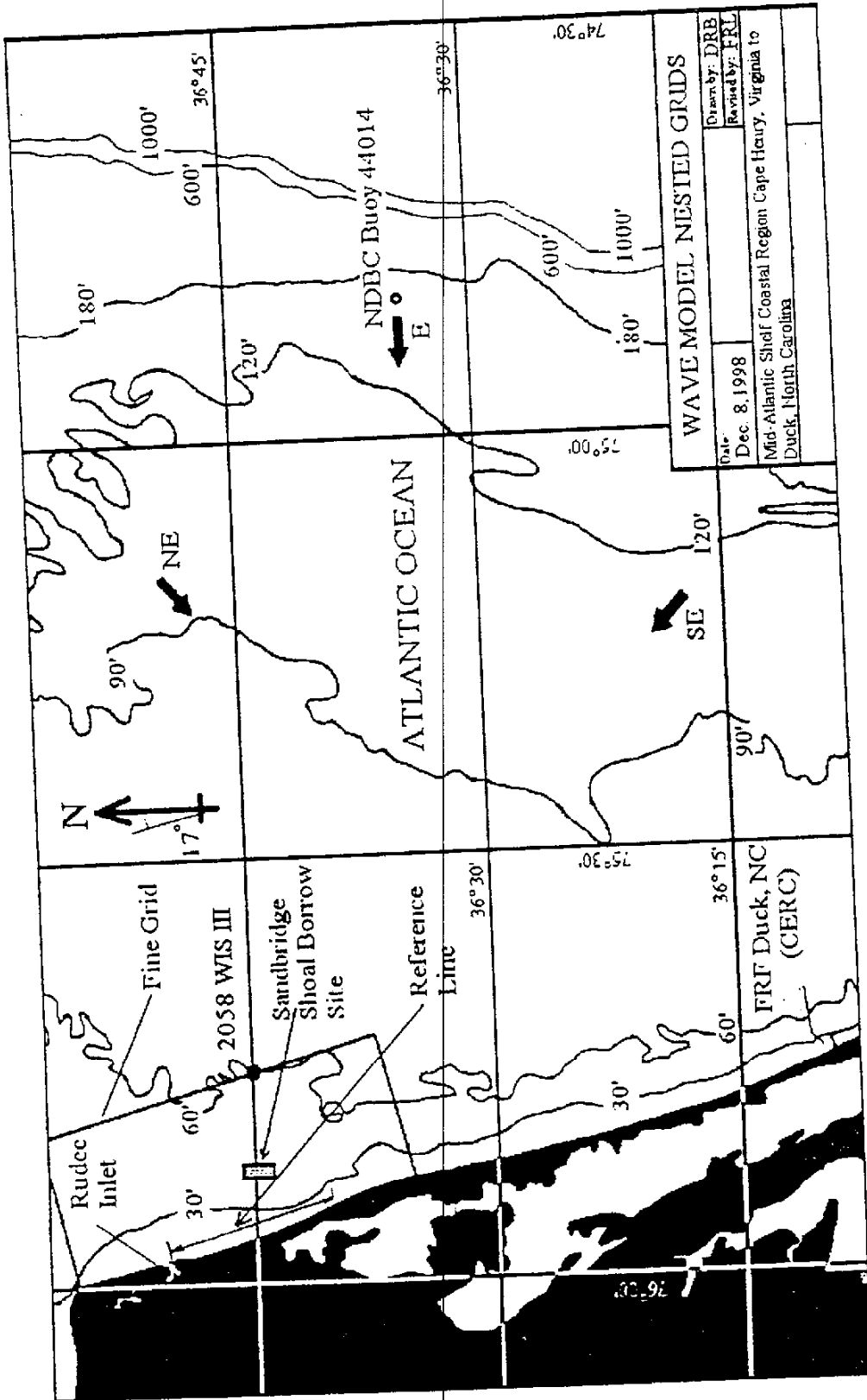


Fig. 11 The study area: the mid-Atlantic Ocean, coastal shelf region off southeastern Virginia extending from the entrance to Chesapeake Bay to the Corps', FRC, Duck, NC.

Wave hindcast information for 20 years periods is available for the locations shown in Figure 12 as determined by the US Army, Corps of Engineers, CERC for the US Atlantic coast (Brooks and Brandon, 1995) for the period 1976-1993 (18 years) and updated for the 20 year period 1976-1995. The most applicable is the Wave Information Study, WIS 2058 site, and is employed herein. Wave rose diagrams are displayed in Fig. 13 with the coastline oriented as shown. In general, higher, shorter period storm waves from the northeast and east directions prevail, whereas, lower, long period, swell waves come from the southwest also in great numbers (Lonza, 1998). An exceedance frequency analysis of 20 years of hindcast wave heights was performed for over 52,600 wave events (3 hour intervals). The median height was 1.4m (4.6ft) and 99.1% were less than 4m (13.1 ft) for WIS 2058 site. For this study we have employed some measured wave data for model calibration but in general have used the 20 year, wave hindcast "information" to represent the local wave climate.

4.4 Wave Model Calibrations

4.4.1 Previous Work. Calibration of the MIKE21.NSW model results against measured wave data in the Chesapeake Bay has been carried out by Basco and Shin (1996). Grid spacings of 300m by 1200m was employed for the axial direction (310km) and lateral direction (155km), respectively. Use of a total wave direction sector of 120° , directional increments of 10° , a narrow directional spreading index ($n = 64$) and roughness coefficient, k_N of 0.0001 produced results that were in good agreement with measurements taken in the middle of the Bay.

4.4.2 Coarse Grid Model To begin, a relatively crude, coarse grid model with uniform grid spacing of 917m was employed over the 115km by 150km region of the southeastern Virginia ocean region shown in Fig. 14. The MIKE21.NSW model requires the left side to be an offshore boundary so that the orientation of all subsequent results will be with South at the top and the North direction arrow as indicated. Locations of measured wave data at the Corp's FRF in Duck, NC (gauge NC01) and at Virginia Beach (VA01) are also shown for reference. The NDBC buoy station 44014 was employed as the measured, offshore boundary condition and is located in about 50m water depth and 100km offshore of Virginia Beach.

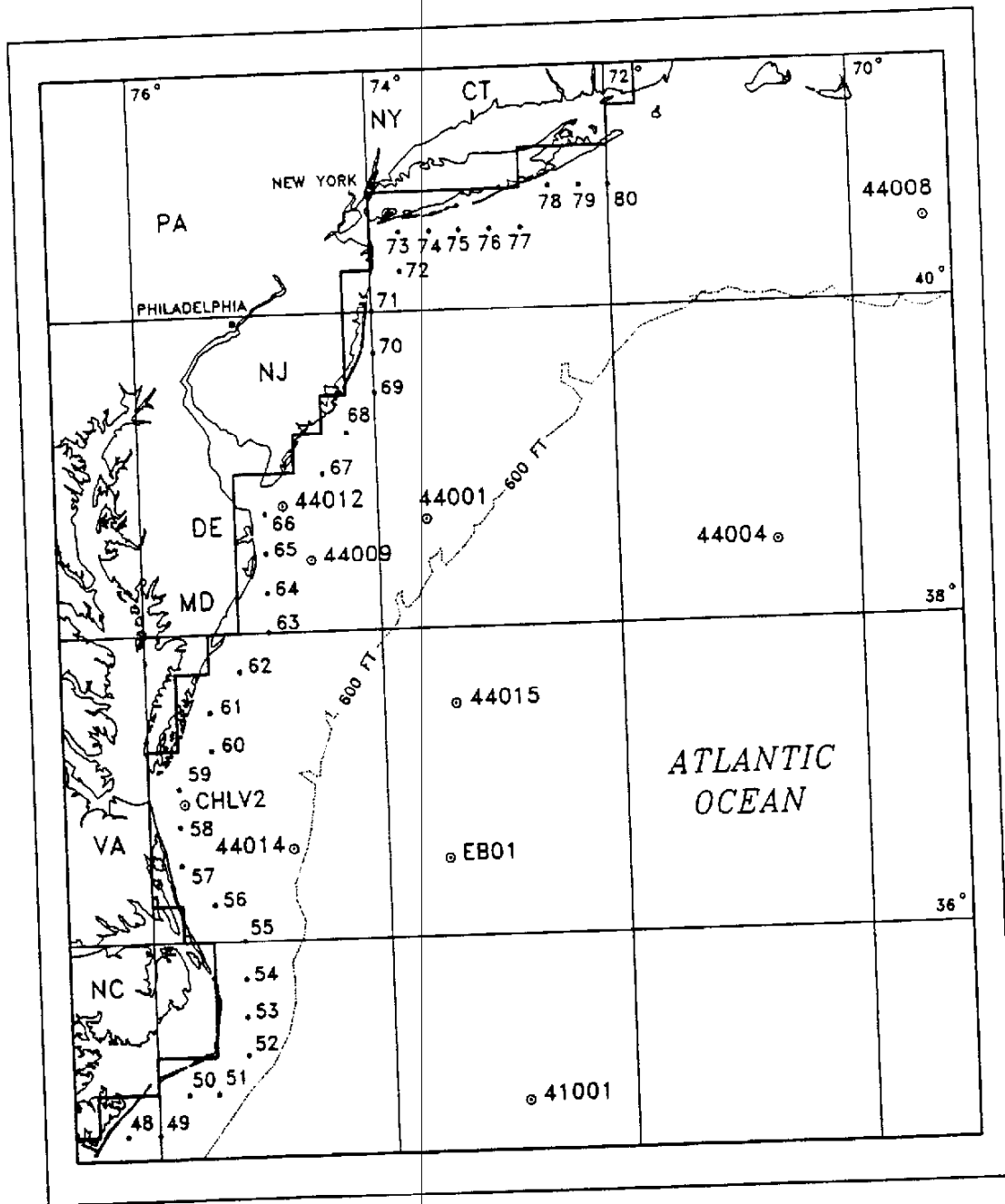
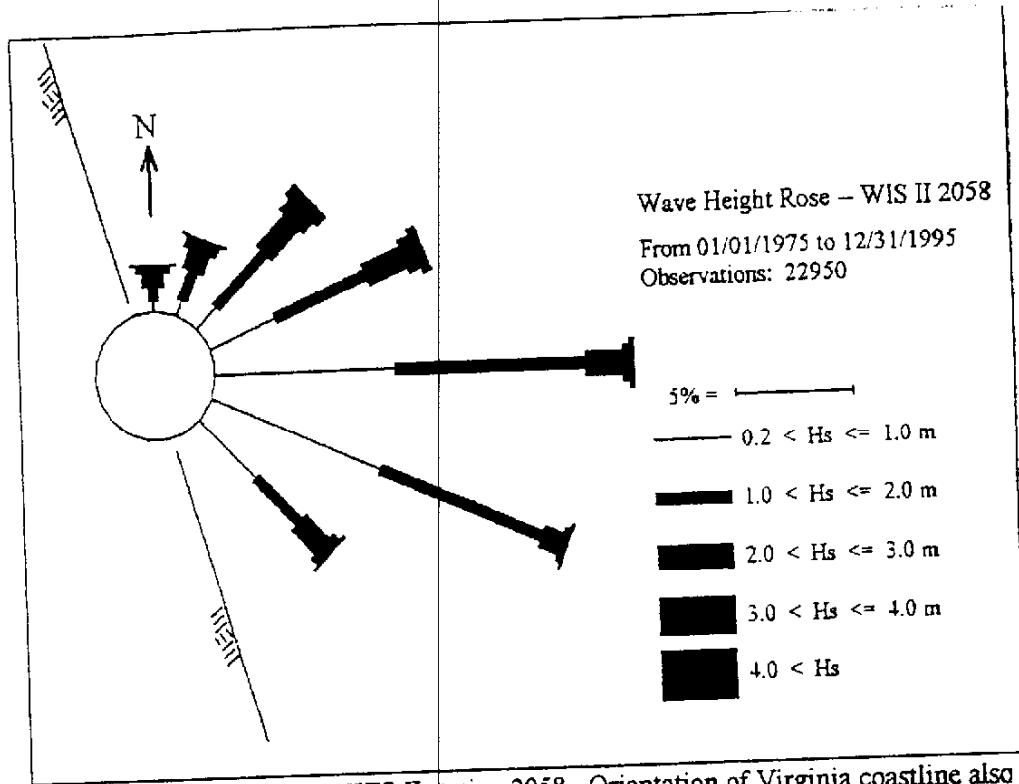
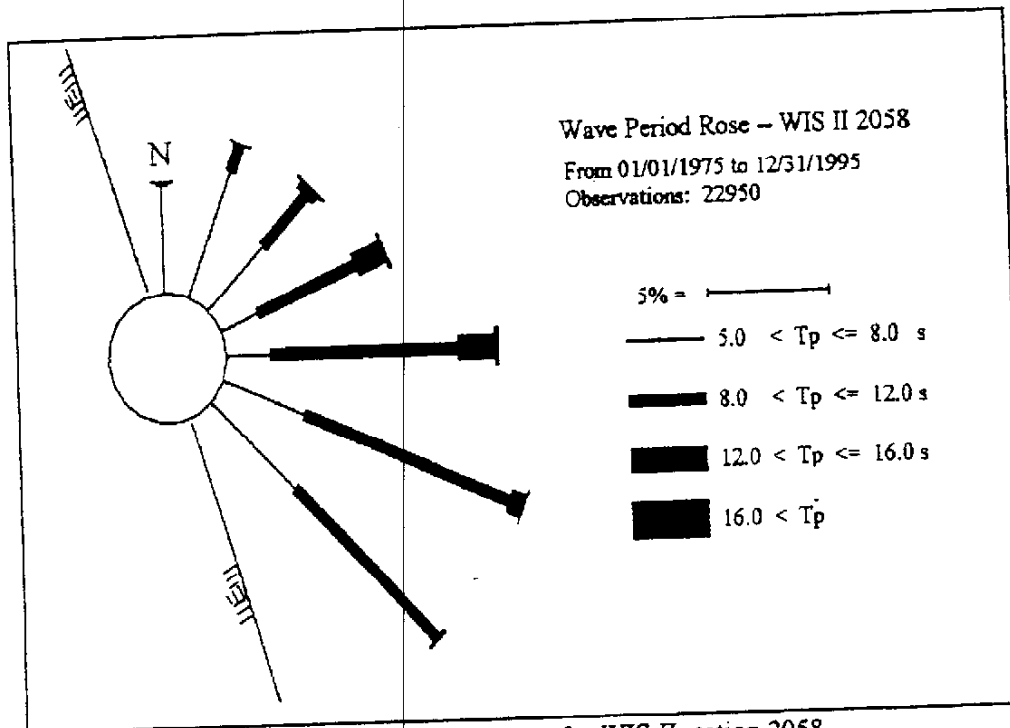


Fig. 12 Location map for Corps of Engineers, WIS stations employed in this study



Wave height rose for WIS II station 2058. Orientation of Virginia coastline also shown.



Wave period rose for WIS II station 2058.

Fig. 13 Wave roses for heights and periods for WIS 2058 station, 20 years, 1976-1995, including hurricanes.

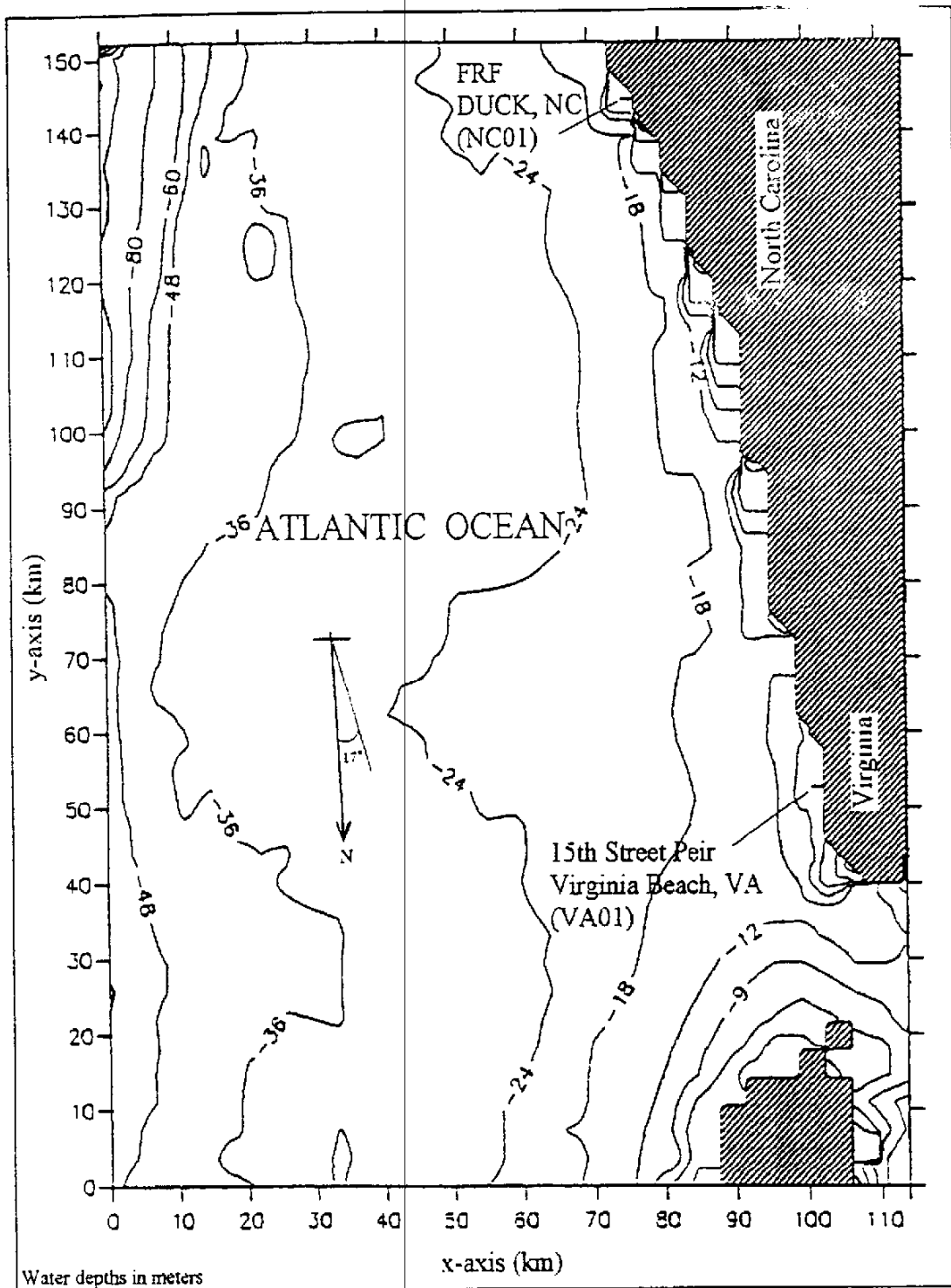


Fig. 14 Coarse-grid model with uniform, 917m grid spacing.

Three storm wave conditions were employed for calibration as summarized in Table 1. Case A was a few days before hurricane BERTHA (July 1996) moved through the region so that offshore waves were 3.0m with relatively calm local, wind-wave generation. Case B had relatively rare, long period waves of 20 sec with a 10m/s wind field. Three conditions were tested for a storm lasting three days in November, 1996 (Case C) that turned through three directions for the offshore boundary conditions.

The modeled results displayed in Table 1 are for the nearest offshore nodes in the model. The discrepancy between measured and modeled results is partly due to the coarseness of the model grid with spacing on the order of 1km. The measured waves are in 8m water depth where depth-induced wave breaking nearshore is not properly represented in the model node shown for comparison in Table I. A finer grid model is necessary nearshore that includes finer resolution bathymetry than that shown in Fig. 14 taken from NOS bathymetric charts.

4.4.3 Fine-Grid Model. The fine-grid spacing was taken about 20 times smaller ($\Delta x = 50\text{m}$) in the cross-shore direction and 10 times reduced ($\Delta y = 100\text{m}$) parallel to the coast at 17° from true north. Bathymetric survey data were obtained from the Virginia Institute of Marine Science (VIMS, 1996) which included new detailed measurements in the Sandbridge Shoal area. The fine-grid modeled region with selected bathymetric contours is shown in Fig. 15. About 350 nodes were needed to model a 17.5km offshore region and 500 nodes required to cover 50km stretching from the entrance to the Chesapeake Bay (bottom) to the VA/NC border (top). The origin is located at Lat $36^\circ 59' 13.8''$ and Lon- $75^\circ 50' 25.2''$.

The location of the offshore boundary coincided with CERC's Wave Information Study, WIS 2058 location for hindcast wave information in about 18m water depth. In this way, the fine-grid model could be used for both a fine-grid calibration using measured wave data and the study of the dredging effects on the hindcast wave climate.

A comparison of measured wave data and modeled results for the fine-grid using the same wave cases is displayed in Table II. The coarse grid results were employed along the boundary of the fine grid but were almost identical with the far, offshore conditions. The comparison between measured, spectral, significant wave heights and mean directions versus those obtained with the fine-grid model are quite good for all five examples. The FRF, Duck, NC data was outside the fine-grid model domain.

Table I Comparison of measured and modeled wave height and wave direction for coarse-grid model (Lonza, 1999)

Case	Boundary Conditions				Gauge VA01 (Virginia Beach, VA)				Gauge NC01 (Duck, NC)			
	H _{mo} m	T _p Sec	θ deg	Wind M/sec (dir)	H _{mo} ,m		θ, degrees		H _{mo} ,m		θ, degrees	
					Meas	Mod	Meas	Mod	Meas	Mod	Meas	Mod
A 7/10/96	3.0	13.0	150	0	0.8	2.2	112	132	1.4	2.3	112	131
B 10/31/96	7.5	20.0	77	10 (330)	2.6	4.2	75	85	3.5	6.0	-	79
C1 11/15/96	3.2	9.0	45	12.5 (018)	1.6	2.5	60	70	2.3	3.0	54	65
C2 11/17/96	4.0	13.0	75	7.5 (343)	1.1	3.2	85	82	3.1	4.5	84	80
C3 11/18/96	6.0	16.0	90	4.6 (344)	1.5	3.4	75	86	2.8	5.0	82	80

Table II Comparison of measured and modeled wave height and wave direction for fine-grid model (Lonza, 1999)

Case	Boundary Conditions				Gauge VA01 (Virginia Beach, VA)			
	H _{mo} m	T _p Sec	θ deg	Wind M/sec (dir)	H _{mo} ,m		θ, degrees	
					Meas	Mod	Meas	Mod
A 7/10/96	3.0	13.0	150	0	0.8	1.1	112	116
B 10/31/96	7.5	20.0	77	10 (330)	2.6	2.9	75	80
C1 11/15/96	3.2	9.0	45	12.5 (018)	1.6	1.8	60	64
C2 11/17/96	4.0	13.0	75	7.5 (343)	1.1	1.4	85	89
C3 11/18/96	6.0	16.0	90	4.6 (344)	1.5	1.9	75	81

The following model parameters and calibration coefficients were therefore employed for all subsequent runs of the MIKE 21.NSW model.

- Directional Spreading

$$n = 8 \text{ (spreading index)}$$

$$\text{DWD} = 45^\circ \text{ (maximum deviation, mean wave direction)}$$

$$N = 19 \text{ (number of wave directions)}$$

$$\Delta\theta = 5^\circ \text{ (spreading angle increments)}$$

- Bottom Friction

$$kN = 6.3 * 10^{-4} \text{ (Nikuradse roughness parameter)}$$

- Wave Breaking

$$\gamma_1 = 1.0$$

$$\gamma_2 = 0.8$$

$$\alpha = 1.0$$

} *Default values (Battjes and Stive, 1985)*

A detailed, complete “calibration” of the model for all possible wave conditions was beyond the scope of this study. The above parameters and coefficients are expected to produce reasonable results for comparison of wave conditions before and after dredging the Sandbridge Shoal.

4.5 Wave Climate Change

4.5.1 Area or Reference Line. Fig.15 also displays the parallel-piped outlines of the two regions designed for sand mining the borrow site as detailed in Section 4.7 below. Waves passing over this region from all offshore directions will refract and shoal further landward to influence a large nearshore, shadow region. Wave climate “change” takes place within the shadow area. The solid, black line (along the 6.5m depth contour) could be employed as a “reference” line to quantify wave climate change resulting from dredging the borrow site. Use of one line to quantify change rather than the entire shadow area greatly simplifies the quantification of change. And, if most of the waves break landward of this line, all the change is *linearly* modeled by the climate. Therefore, we have chosen to employ a strategically located reference line to quantify wave climate change.

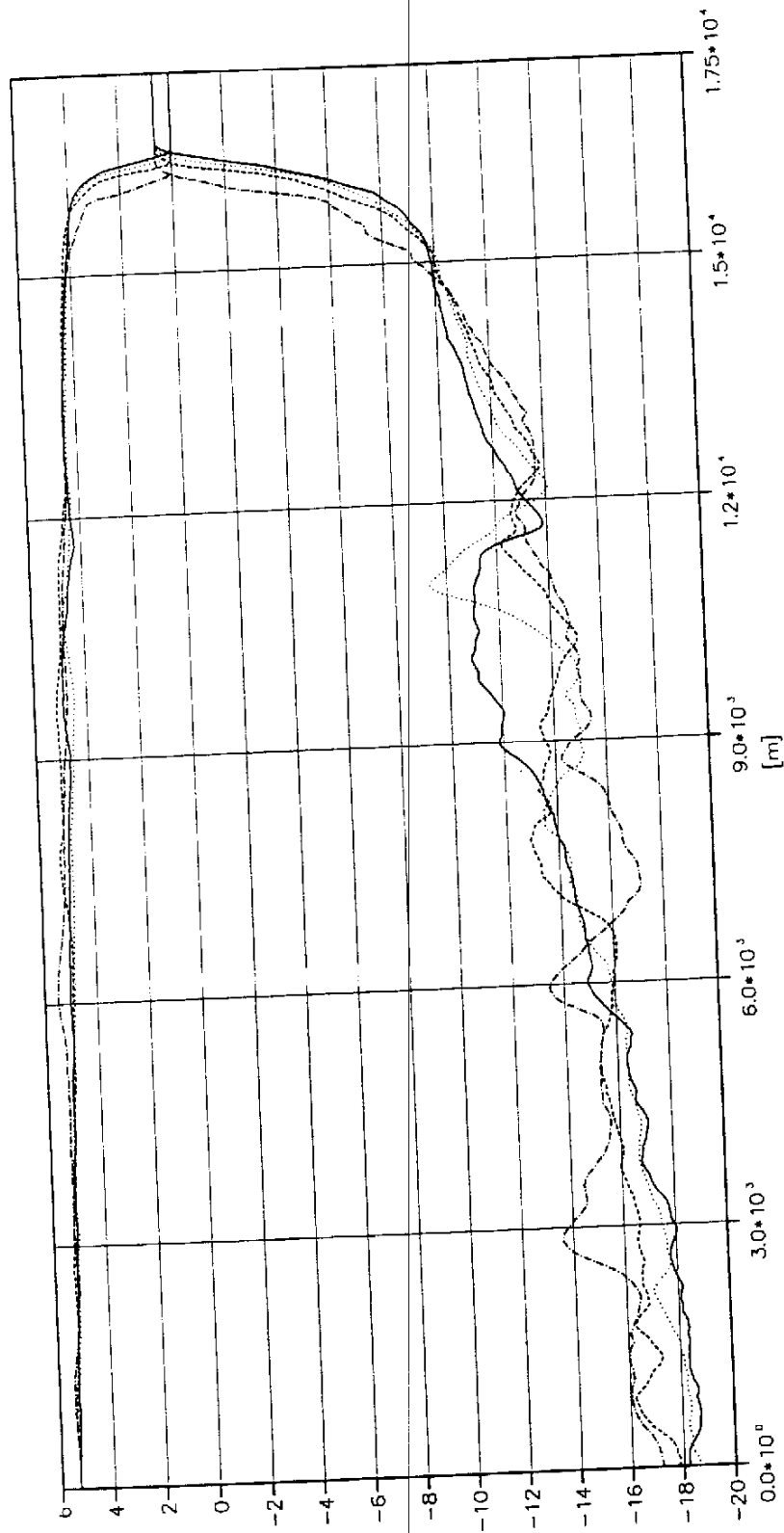


Fig. 16 Wave height variation across the beach profile at four locations (corresponding bathymetry also shown) for $H_{mo} = 5.3\text{m}$, $T = 19\text{s}$, $\theta = 83^\circ$ as calculated by MIKE21.NSW model

4.5.2 Location of Reference Line. As shown in Fig.16, for one large, long period wave condition ($H_{mo} = 5.3\text{m}$, $T = 19\text{s}$, $\theta = 83^\circ$) as input, boundary condition along the fine-grid boundary, most of the wave energy is lost due to wave breaking close to shore at shallow water depths which are also indicated. Each of the four wave height profiles and depth contour profiles have similar line symbols and are equally spaced over a 10km reach directly landward of the sand borrow site (Fig. 15). For irregular, spectral representation of wave characteristics, the steepness and depth-controlled wave breaking criterion of Battjes and Stive (1985) produces these realistic, wave energy decay and breaking curves which are far different than classical, shoaling and point breaking of monochromatic waves of linear wave theory. For this wave example, "breaking" begins (large gradient of wave energy change) in about 7-7.5m water depth. Larger waves "break" further offshore. Eight examples were studied for wave heights ranging from 3.8 to 6.9m and a range of periods but shore normal direction. It was learned that waves with H_{mo} equal or greater than 4.0m break seaward of the 6.5m contour. Therefore, as shown in Section 4.3, this means that 99.1% of the waves in the total wave climate break *landward* of the 6.5m contour.

Wave transformation processes as modeled are essentially *linear* seaward of the 6.5m contour for 99.1% of the waves in the 20 year wave climate. This means that a unit wave height of 1.0m can be used at the boundary to represent all wave heights in the climate. Wave transformation processes for the 1.0m wave will produce a wave multiplier "coefficient" along the 6.5m contour that can be simply multiplied by the actual wave height at the boundary to produce the same variation in wave height along the 6.5m contour that the model would produce for each, actual wave height. In this way, the wave climate variation is simplified to wave period and direction variability for a unit (1.0m) wave height. The 6.5m depth contour line has been chosen as the "reference line" for this study.

4.5.3 Length of Reference Line. In the thesis of Lonza (1999) a 10,000m long reference line was employed centered along the mid-section of the borrow site. The wave energy density variation along the reference line (see next section) was calculated for existing (before) and dredged (after) conditions of the bathymetry in the borrow site. It was found that the change in wave energy density at the ends of the reference line did not return to zero. This simply means the reference line of 10,000m was too short. The shadow zone of wave change produced by the dredging extended beyond the ends

of the 10,000m reference line. It was then determined that a 20,000m long reference line (Fig. 15) was required and used for all results reported herein. Note that this length about 3-4 times longer than the lateral dimension of the borrow site. The change in wave height before and after dredging returned to zero at both ends of the reference line for all periods and directions in the wave climate.

4.6 Wave Energy Variability

4.6.1 Condensing the Wave Climate. A Corps of Engineers, CERC software program called WHEREWAV was employed to condense the wave climate to seven period bands (5-23 sec) and seven direction bands that accounts for practically all the important waves in the hindcast wave climate. The WHEREWAV results are found in Appendix A. Waves with periods less than 5 sec were neglected because they are negligibly influenced by bottom variations. There were no waves with period greater than 23 sec. For a shoreline orientation of 343 degrees azimuth, the angle bands relative to shore-normal of 84.25 to 90° and -73.25 to -90° were also neglected. Waves from these very oblique angles are rare and not modeled accurately for the required boundary conditions in MIKE21.NSW. This produced 49 period/direction combinations.

The software program WHEREWAV distinguishes between "primary" or "sea" wave conditions and secondary or "swell" waves as found in the wave hindcast model. For 3-hr intervals over 20 years a total of 58440 wave records are available. We have employed the 47,920 primary wave events for this study with the difference due to offshore traveling wave events (10,515) and 5 calm wave events. Neglect of the two period bands and two angle bands eliminated 2449 wave events so that 45,471 (94.9%) of possible wave climate events were studied in this analysis. These include all waves with periods greater than 5 seconds that propagate across the Sandbridge Shoal and can be influenced by dredging the shoal. Table III displays the distribution of the number of wave events in the seven period and seven direction banks selected. The period and directions listed are at the mid-point of each band.

Note that the WHEREWAV results (Appendix A) do not sort the waves in wave height bands. If 10 wave height bands were employed, a total of 490 (49 * 10) wave conditions would need to be modeled for both before and after dredging conditions. This would mean 980 numerical model runs and a very time consuming process. Locating the reference line in 6.5m water depth permitted a unit wave height (1.0m) to represent all the possible wave height conditions. This reduced the number of model runs needed by a factor of 10. Consequently, 98 (49 * 2) model runs were required to quantify the before and after dredging change on the wave climate. But 49 period/ direction

combinations and their change along the reference line is still a large number of individual conditions to digest.

4.6.2 Condensing the Wave Energy Climate. An example of the wave height multiplier coefficient variability along the reference line for one case ($H = 1.0\text{m}$, $T_p = 11.4\text{sec}$, $\theta = 86.3^\circ$) is shown in Fig 17(a) for both before (dotted) and after (solid) dredging the shoal. Full details on the borrow site dredging arc in the next section. The multiplier coefficient varies between about 1.12 and 0.85 for this example. Clearly, the wave height is lower, after dredging, directly landward of the borrow site (middle zone of reference line), larger on both sides, but then returns to the same multiplier coefficient at both ends of the reference line. Note, that the wave height varies considerably near the ends of the reference line, but the wave height change near the ends is zero, as required for a meaningful length of a "reference" line. Fig. 17(b) displays mean wave angle variability crossing the reference line. The change for before and after dredging shows a discernable trend but again the change is zero near both ends, as desired. Forty-eight similar plots for all other period/direction combinations are possible.

To combine all the possible wave height cases for each period/direction combination, Lonza (1999) calculated the wave energy density, e defined as

$$e = \frac{E}{L} = \frac{1}{8} \rho g H^2 \quad (14)$$

where:

E = the wave energy for a given period

L = the wave length associated with the given period and water depth

ρ = fluid mass density

g = gravity constant

H = wave height

Each boundary condition wave height in the 49 period/direction bins (Table III) was first multiplied by the coefficient along the reference line and then Eqn (14) applied to find $e(x)$. The energy was then summed and weighted for all waves in each period/direction band and the change is energy density for before and after dredging conditions plotted for 49 period/direction combinations. Lonza

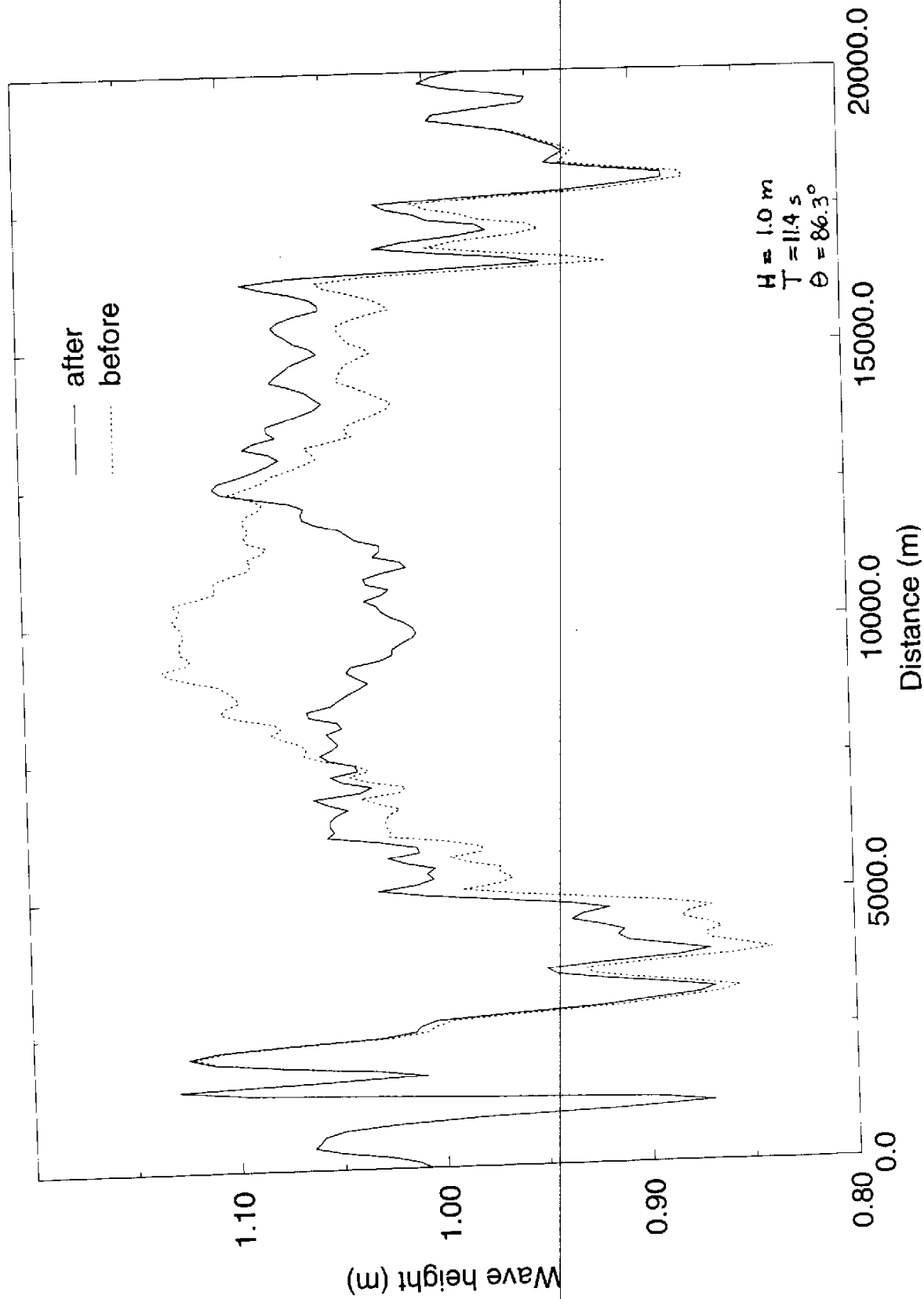


Fig. 17(a) Example, unit height "multiplier" coefficient variability along the reference line for before (dotted) and after (solid) dredging the shoal for one wave case.

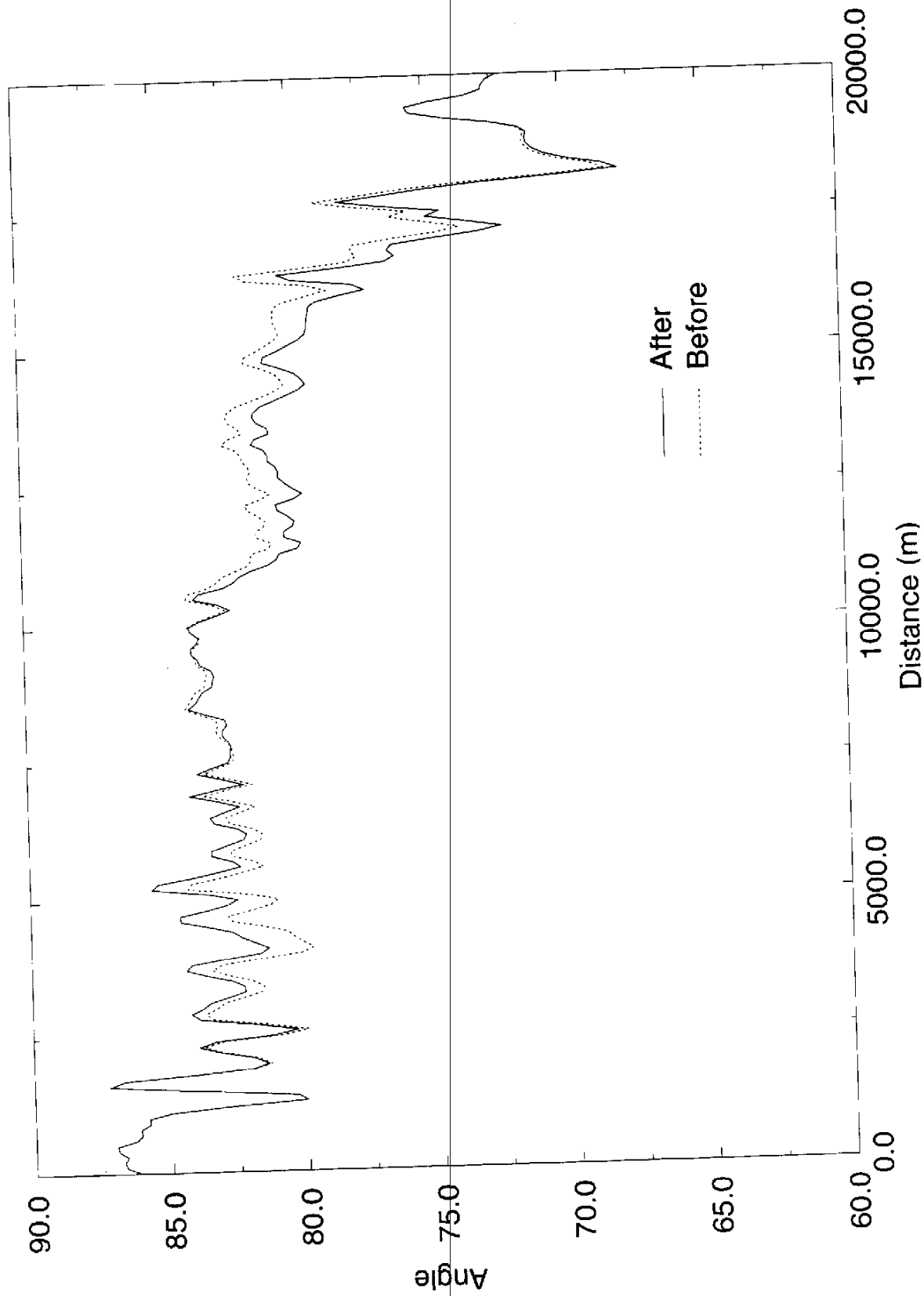


Fig. 17(b) Example variability in mean wave angle, α crossing the reference line for same case.

Table III Number of wave events for chosen wave direction-wave period bands, WIS 2058, 20 years, 1976 -1995, including hurricanes

<u>Direction</u> →	359.76	23.0	45.4	70.4	86.3	111.8	132.8
<u>Period</u> ↓	970	635	690	689	810	661	585
5.44	8	22	236	1155	2798	4613	1126
7.58	0	1	37	1953	5062	5187	548
9.46	47	64	43	1281	5928	1627	150
11.43	0	0	1	281	4784	358	4
13.39	0	0	0	14	2030	112	0
15.37	0	0	0	1	862	98	0
18.03	0	0	0				
Total	45471						

(1999) displays 49 energy density plots in his thesis.

Finally, to condense all the 49 combinations, we have used Eqn (14) to calculate total wave energy, E along the reference line. Linear wave theory was employed to calculate the local wave length, L for each wave period and at water depth, $d = 6.5\text{m}$. Hence, we employed

$$E(x) = \frac{1}{8} \rho g H^2(x) L \quad (15)$$

and used the number of waves at each height and in each period/direction bin (Table III) to find the weighted, total energy, $E(x)$ along the reference line. In this way, we have condensed the 20 year wave climate consisting of 45,471 wave events into one curve that displays total, weighted wave energy along the reference line for all wave heights, wave periods, wave directions and number of wave events. To the writer's knowledge, this technique has not been applied before to summarize a wave climate. Before examining the $E(x)$ variability along the reference line, we shall first define the Sandbridge Shoal borrow site in detail.

4.7 Sandbridge Shoal Borrow Site

4.7.1 Split Zones for Dredging. The original borrow site for the Dam Neck beach nourishment project in 1996 covered about 780 acres on the east end of Sandbridge Shoal (Fig. 18). Figure 19 displays the bathymetry in color with the large green area offshore as the shoal. A three-dimensional, close up view looking to the northwest direction and more resolution in the colors, clearly displays the shoal area (orange, brown) in Fig. 20.

It was unfortunate, that on the very first day of dredging, an important underwater cable belonging to the U.S. Navy was hit and severed. Further operations were delayed until a wide zone was declared as a "prohibited area" for all future excavation. The Sandbridge beach nourishment project in 1998 specified the areas "B" and "BB" and the prohibited area as shown in Fig. 21 (from Corps of Engineers, 1998, Sheet C 50). In this study we have used this location and expanded it to meet the 25-year and 50 year beach renourishment needs of the region.

4.7.2 Volumes Required for Design Life. The design life is 25 years for the Dam Neck beach and 50 years for both Sandbridge beach and the Tourist beach of the City of Virginia Beach. The maintenance requirements for beach renourishment have therefore been estimated for both 25 and 50 years for all three beaches. We have employed design information in Basco and Cummings,

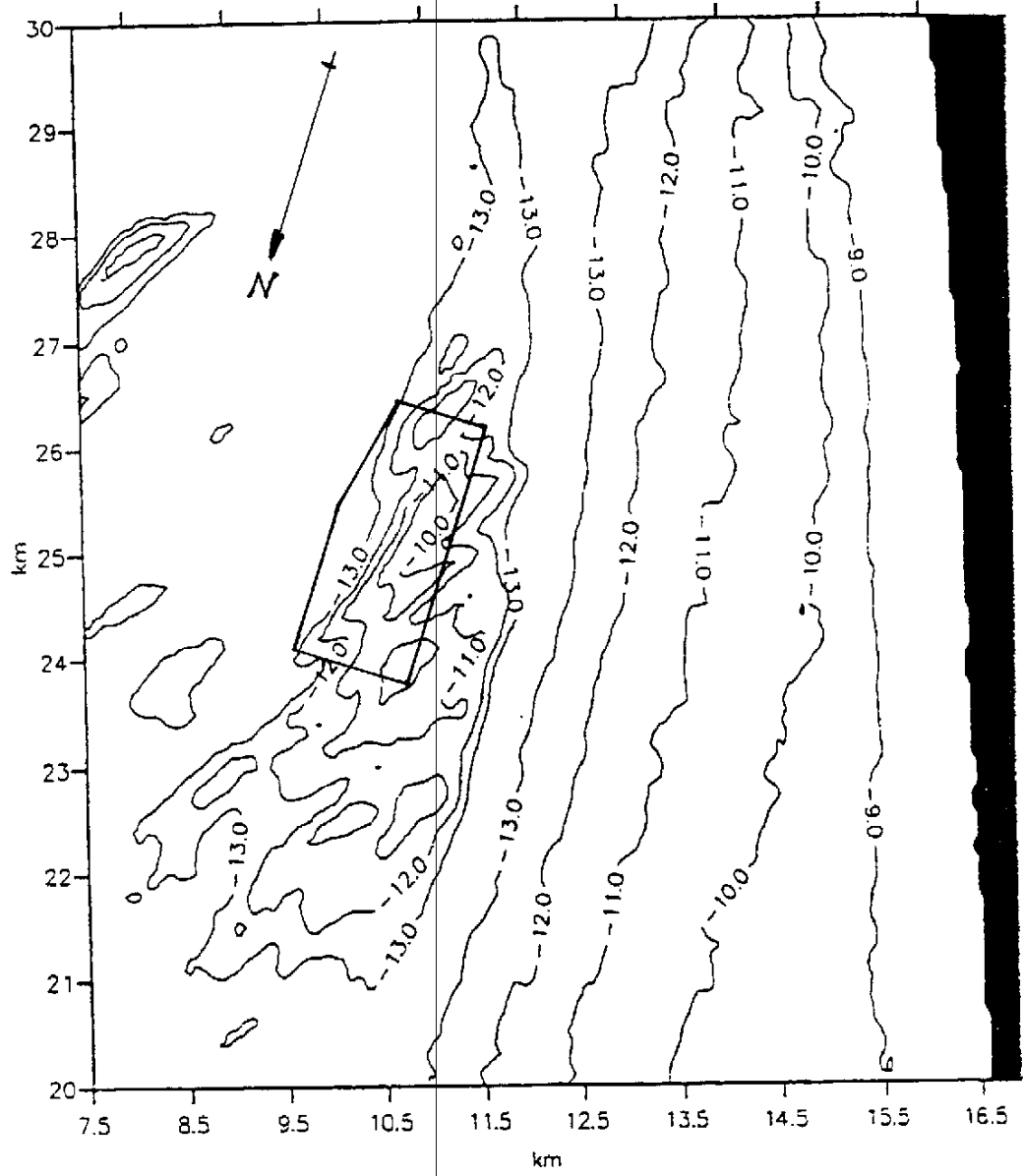


Fig. 18 Original borrow site for Dam Neck beach nourishment project in 1996 covering 780 acres on East side of shoal.

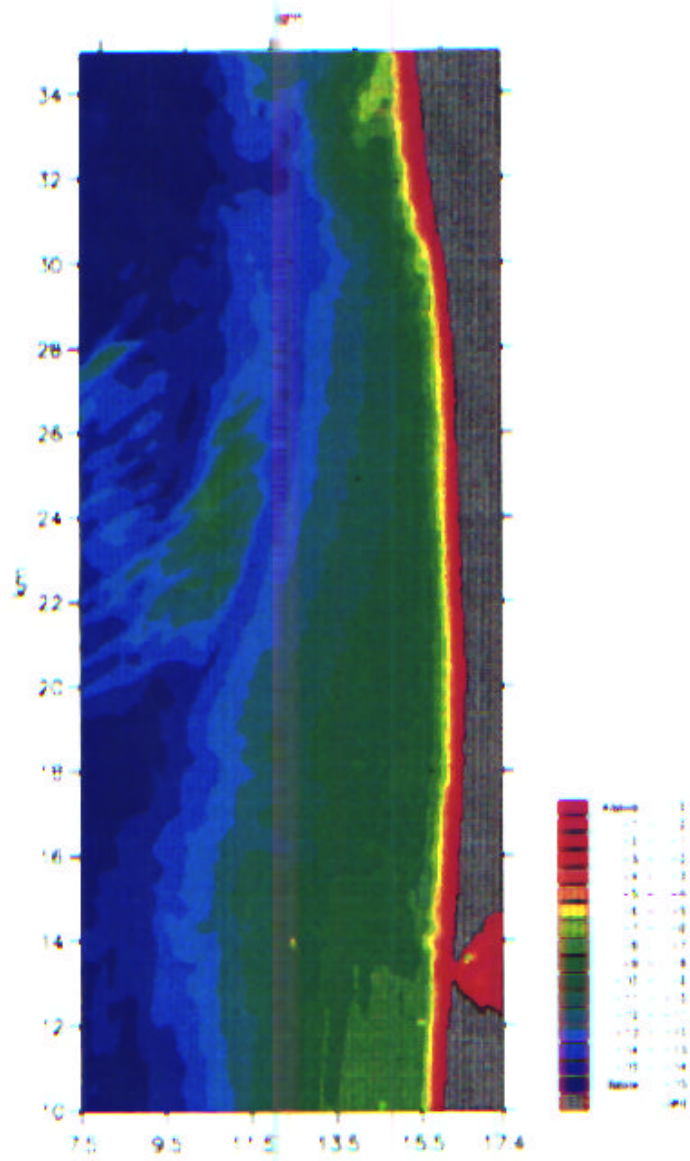


Fig. 19 Color display of bathymetry in fine-grid model

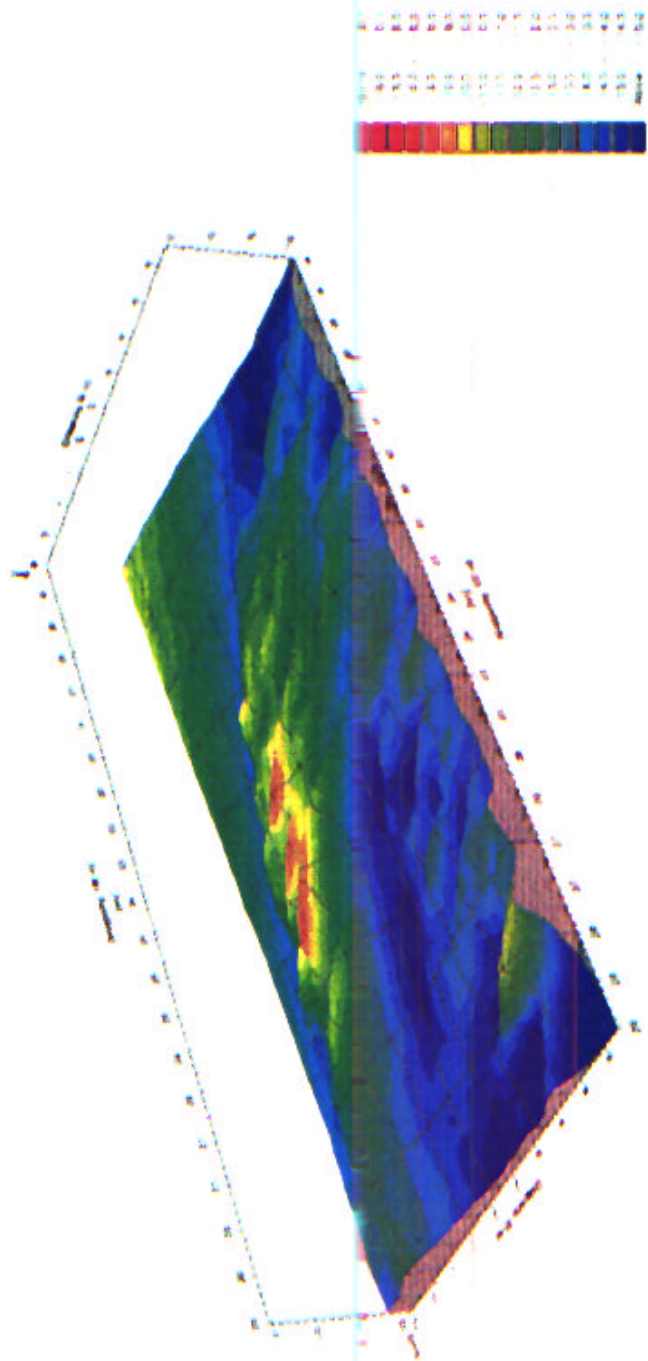


FIG 20 Increased color resolution and close-up view looking northwest of the Sandbridge Shoal (orange, brown)

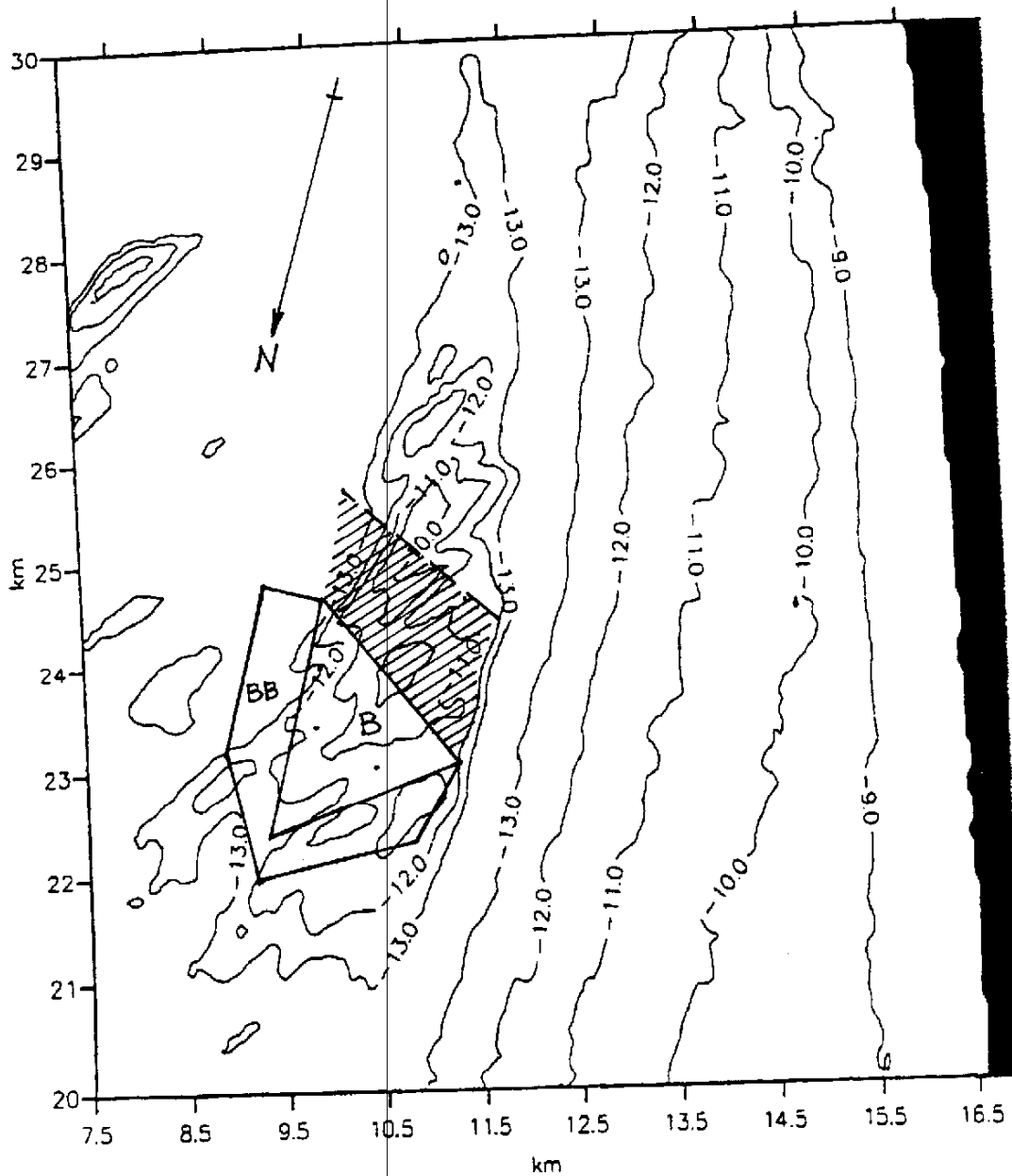


Fig. 21 Designated, sand borrow site boundaries for the Sandbridge Beach nourishment project in 1998 (from Corps of Engineers, 1998 b, sheet C50) and prohibited region

(1995); COE (1992) and COE (1994) to obtain expected fill life and re-nourishment intervals (years) for Dam Neck, Sandbridge and the Tourist beaches, respectively. We have also used the actual sand volumes dredged from project records (Basco, 1998; COE, 1998) for the Dam Neck and Sandbridge fill volumes, initially placed. Table IV summarizes the results.

Table IV Sand Volumes for Design Life

No.	Project Name	Initial Volume cy (million)	Interval years	Maintenance Volume Per Cycle cy (million)	Total Volume, cy (million)		
					25 yrs	50 yrs.	Ranks
1	Dam Neck	0.755M	10 - 12	0.7M	1.5M	3.0M	
2	Sandbridge	1.10M	2	0.5M	7.1M	13.6M	
3	Subtotal	2.855M			8.6M	16.6M	Probable
	Tourist beach	5.0M	3	0.765M	11.1M	17.2M	
	Total	7.855M			19.7M	33.8M	Possible

Based on these estimates the total, possible sand volumes required are 20M and 34M cy for 25 and 50 year periods, respectively. However, the sand requirement needs of the Tourist beach could come from other, nearby sand sources such as the Thimble Shoal and Atlantic Entrance channels for deep draft navigation. Therefore, the probable sand requirements are 9M and 17M cy for the 25 year and 50 year need of Dam Neck and Sandbridge beaches. These estimates consider each project separately and neglect the regional, sand volume movements alongshore between beaches, so are conservative.

To meet these needs, we have developed two, split borrow sites A & B as depicted in Fig. 22 with a relatively flat bottom contour at -50ft (15.24m). The side slopes are 2:1 and we assume no resettlement of sand over the long term. Fig. 23 is a plan, color view of the split borrow area and Fig. 24 is the perspective, color picture of the Sandbridge Shoal, dredged borrow area employed in this study. The total volume of sand excavated is 4.34×10^7 cy. Area A covers 1095 acres and B covers 1465 acres totaling 2560 acres. The volume of material removed from A is 20.9 M cy and from B is 22.5 M cy totaling 43.4 M cy.

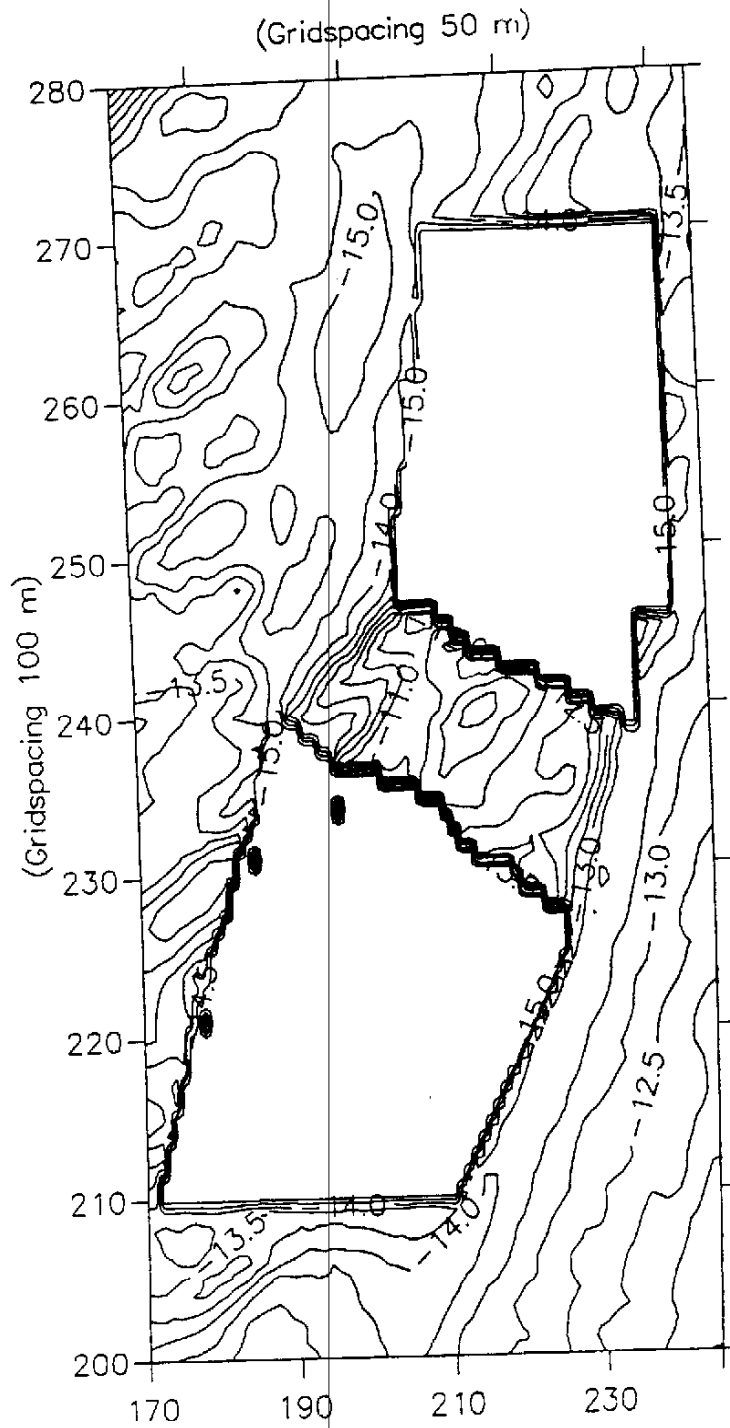


Fig. 22

Split borrow sites in the Sandbridge Shoal to accommodate prohibited region and long-term (50-year) dredging volume requirements

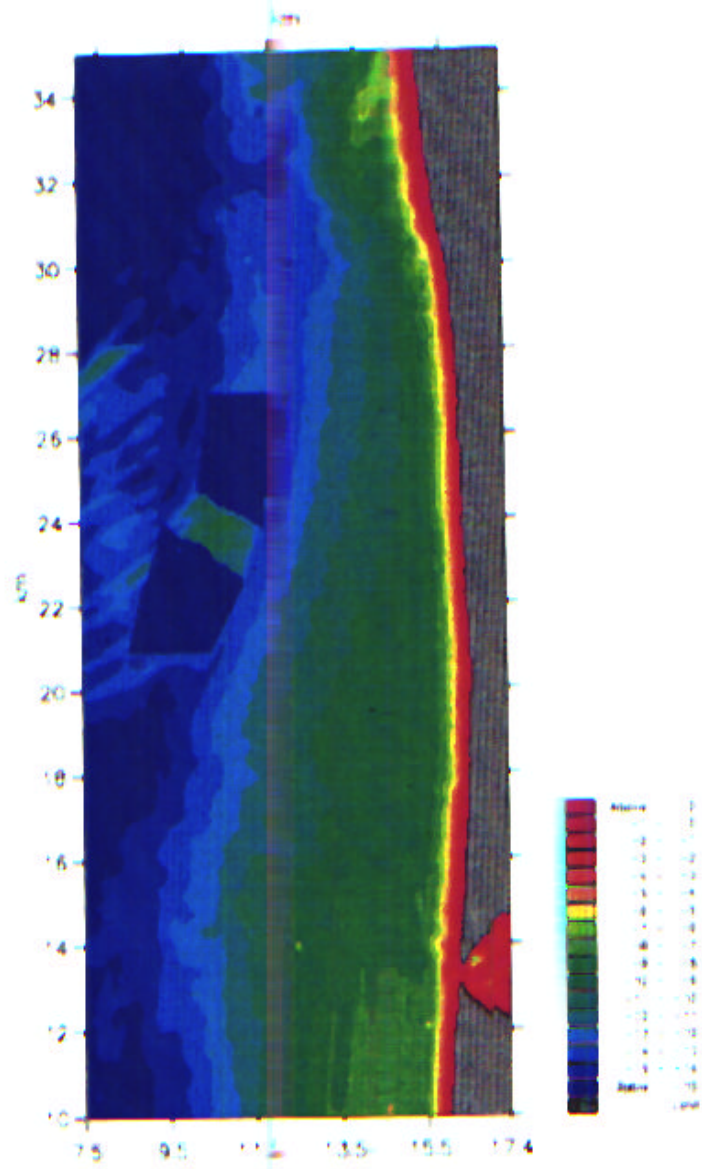


Fig. 23 Plan, color view of the split borrow site in the fine grid model

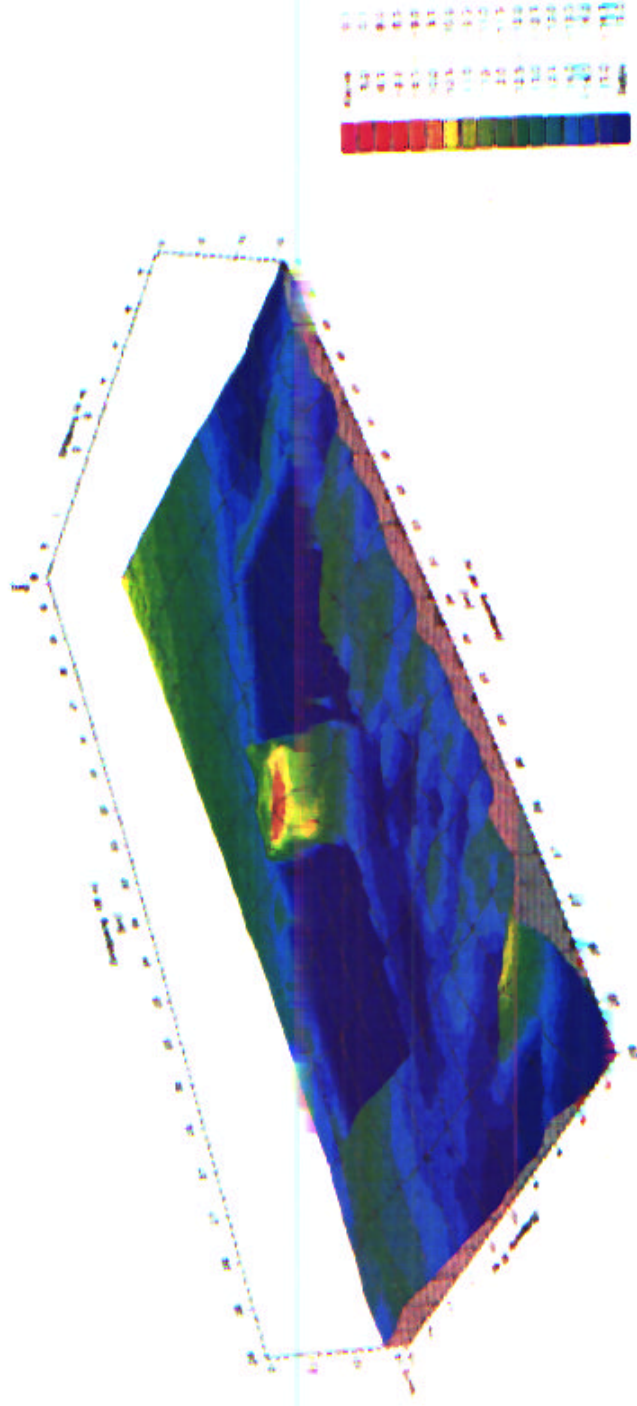


Fig. 24 Closer view, perspective, color picture of the Sandbridge Shoal, dredged borrow area employed in this study

4.8 Wave Energy Change

As discussed above in Section 4.6, we have employed Eqn. (15) to condense 45,471 wave events into one curve that displays total, weighted wave energy along the reference line for all wave heights, wave periods, and wave directions. These results are displayed in Fig. 25 as the solid line for existing, before dredging bathymetric conditions. The total integrated wave energy over the 20,000m reference line is $4.5433 * 10^9 \text{ kg.m}^2/\text{s}^2$ but varies considerably along the reference line.

We then use the results of Section 4.7 and modify the bathymetry to accommodate the long term, sand nourishment needs of the region. The same wave climate is introduced and $E(x)$ again computed along the reference line and shown as the after dredging, dotted line in Fig. 25. As revealed in Fig. 17a for a unit wave height and one wave case, the region directly landward of the borrow site ($7,000 \leq x \leq 12,000\text{m}$) has *less* total wave energy and the side areas have slightly *more* wave energy. The total wave energy remains constant at both ends of the reference line, as required. Total integrated wave energy over the 20,000m reference line after dredging is $4.53156 * 10^9 \text{ kg.m}^2/\text{s}^2$ and only 0.26 percent less than before dredging.

Fig. 26 displays the percentage change in total wave energy in the total climate along the reference line by this technique. Here, we clearly see the impact of the long term dredging of Sandbridge Shoal on the nearshore wave climate. Total energy remains about the same but it's *distribution* is modified by $\pm 10\text{-}15$ percent or more along a 20km distance landward of the borrow site.

Wave direction is also changed by the borrow site dredging. Fig. 27(a) displays before (dotted) and after dredging (solid) wave angles along the reference line for one wave period and direction at the boundary ($T_p = 9.46\text{s}$, $\theta = 86.3^\circ$). The percent difference is shown in Fig. 27(b) with positive meaning a larger angle after dredging. Similar results are presented in Fig. 28(a) and (b) for the same period ($T_p = 9.46\text{s}$) but different wave direction ($\theta = 111.8^\circ$) at the boundary. In both cases, the angle change returns to zero at both ends of the reference line, as desired. Other cases give similar results showing ± 2 percent maximum change in wave angle along the reference line.

We have not attempted to combine all the wave events to determine the weighted average change in wave direction. One possibility would be to employ the alongshore component of the wave induced, radiation stress, S_{xy} along the reference line where:

$$S_{xy} = E C_g \sin \alpha \cos \alpha \quad (16)$$

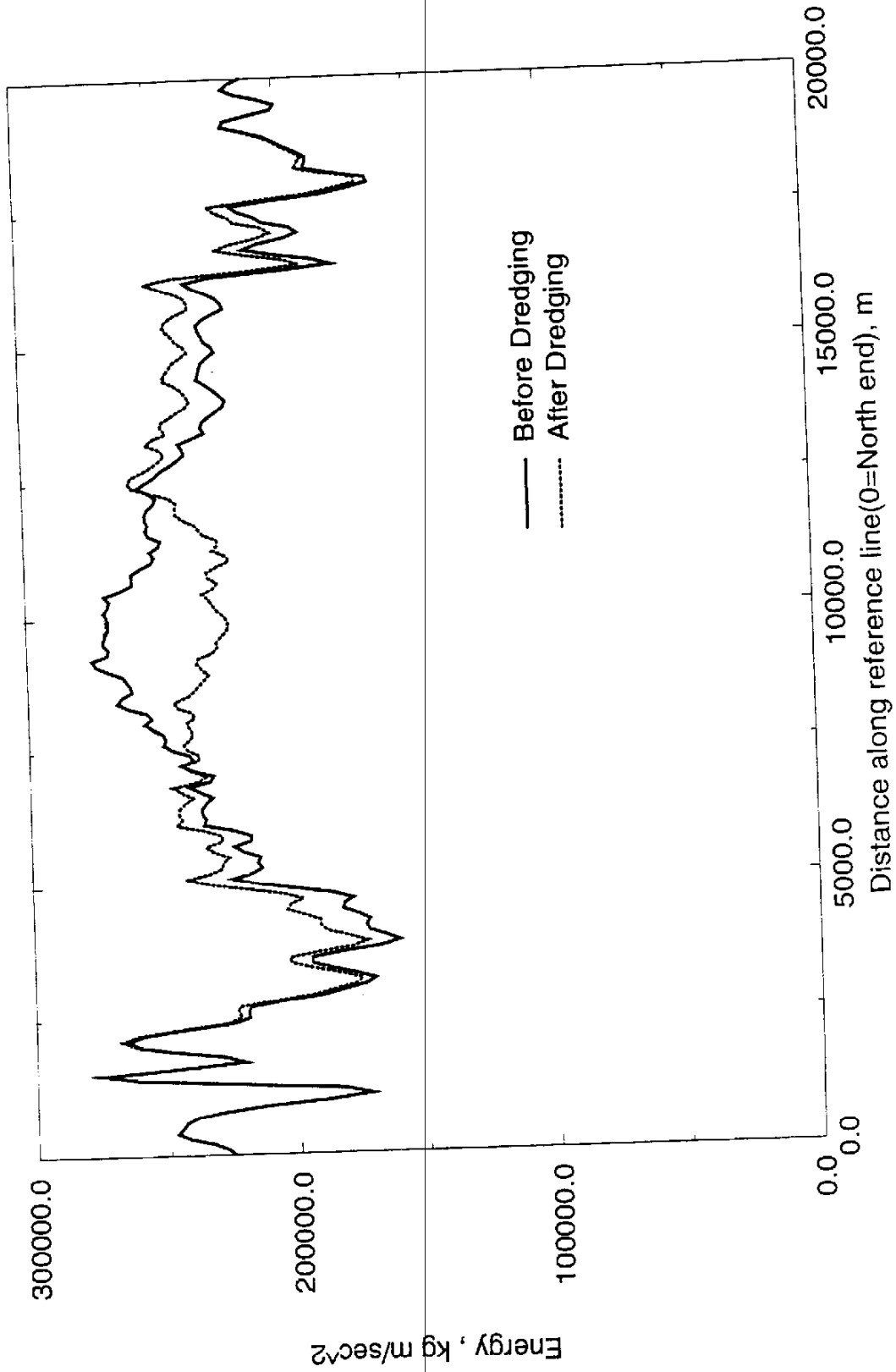


Fig. 25 Total, weighted wave energy variability along the reference line for the WIS 2058 wave climate for before (solid) and after (dotted) dredging.

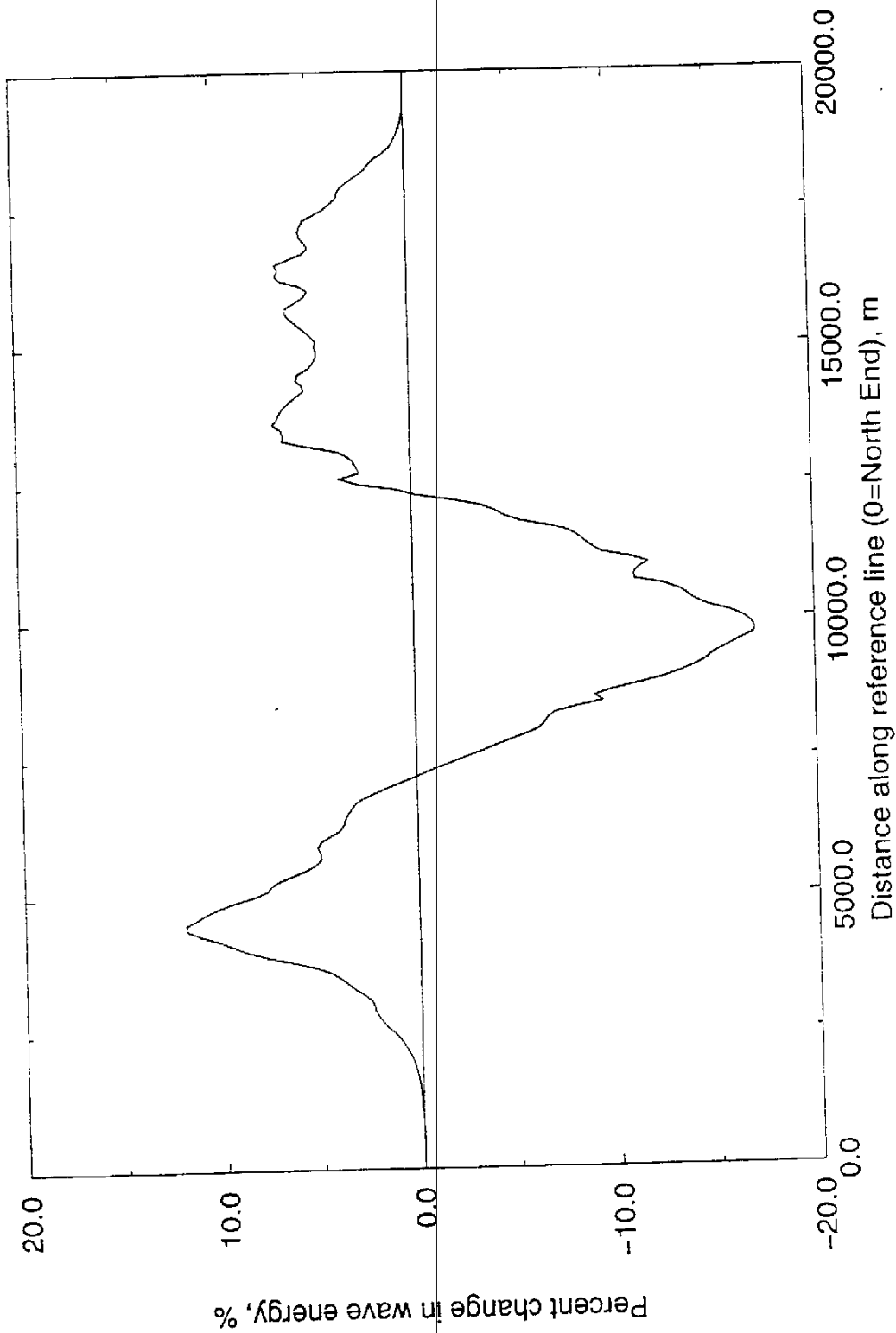


Fig. 26 Percentage change in total, weight wave energy in the wave climate and its variation along the reference line. Positive means a wave energy increase.

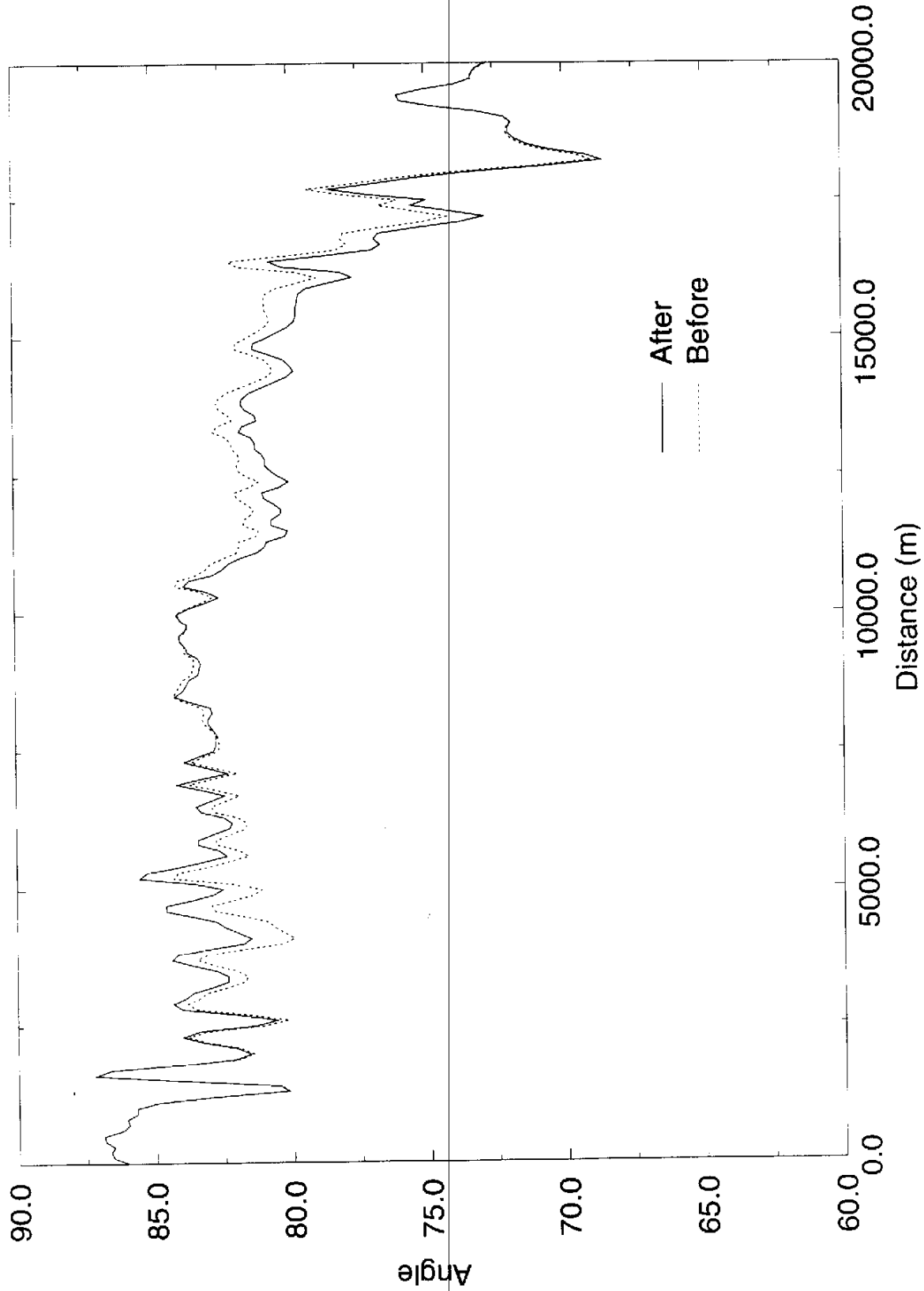


Fig. 27(a) Before (dotted) and after dredging (solid) mean wave angle crossing the reference line for $T_p = 9.46s$, $\theta = 86.3^\circ$

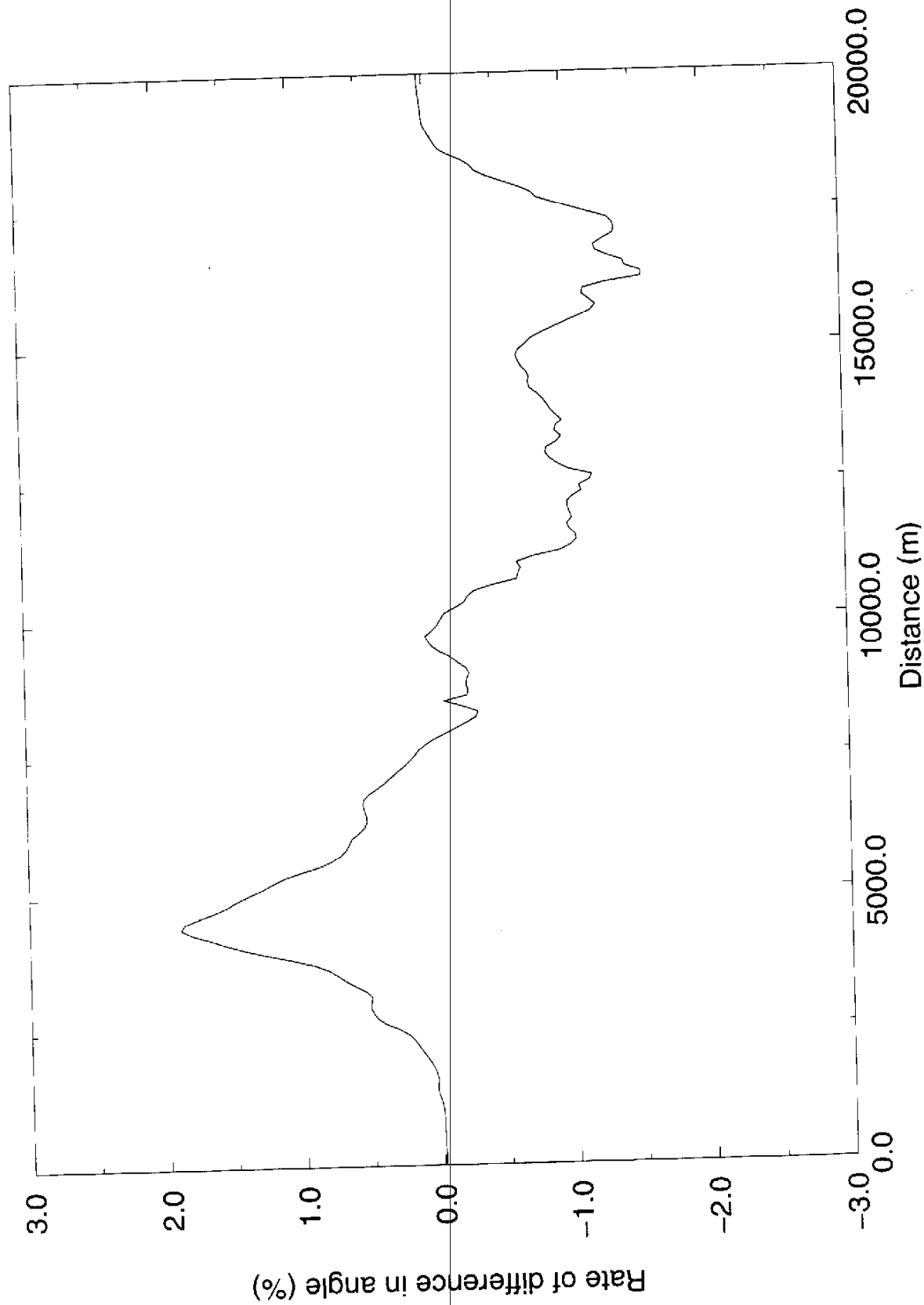


Fig. 27(b) Percent change in wave angle along reference line for same wave conditions as (a).

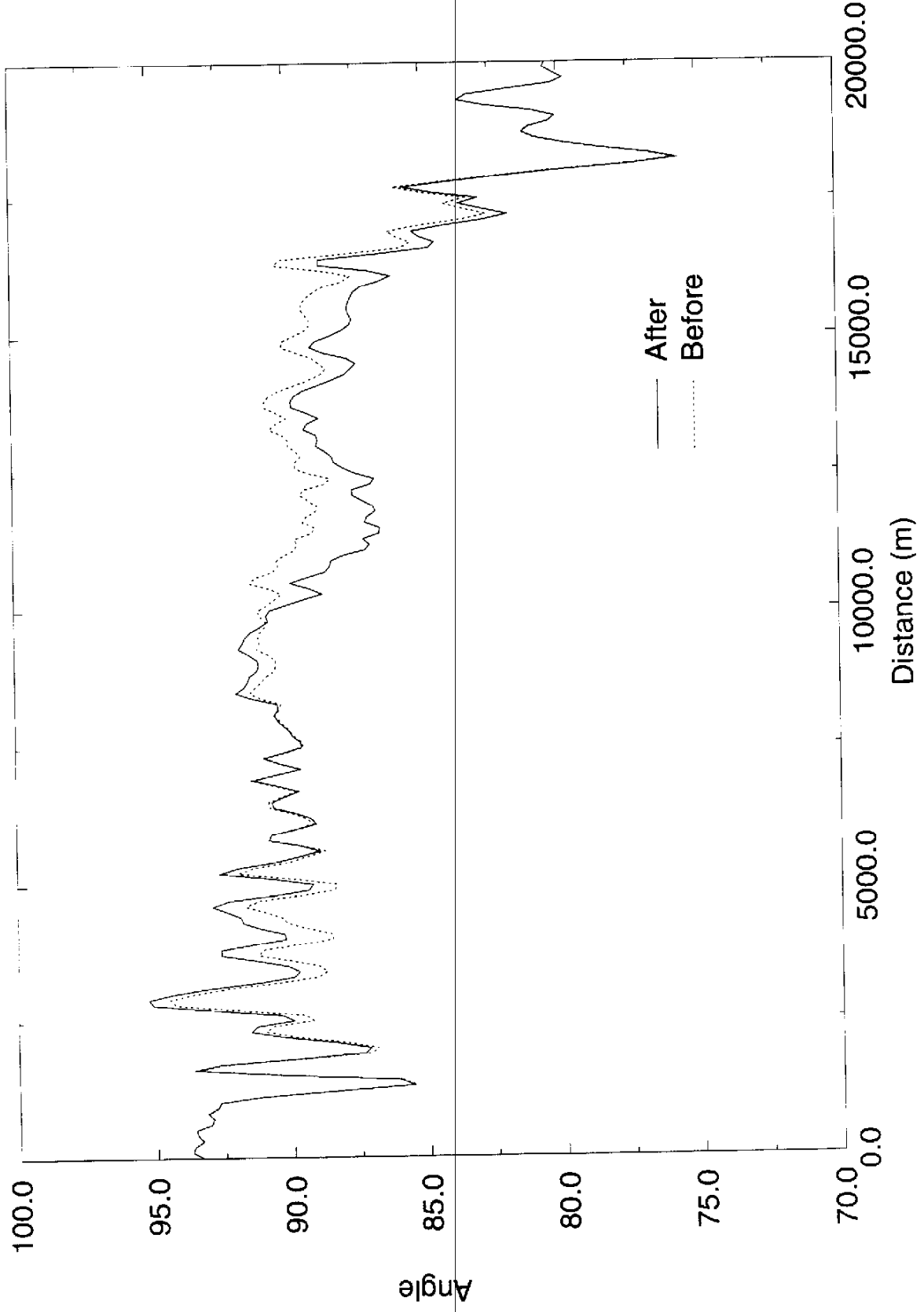


Fig. 28(a) Before (dotted) and after dredging (solid) mean wave angle crossing the reference line for $T_p = 9.46s$ and $\theta = 111.8^\circ$.

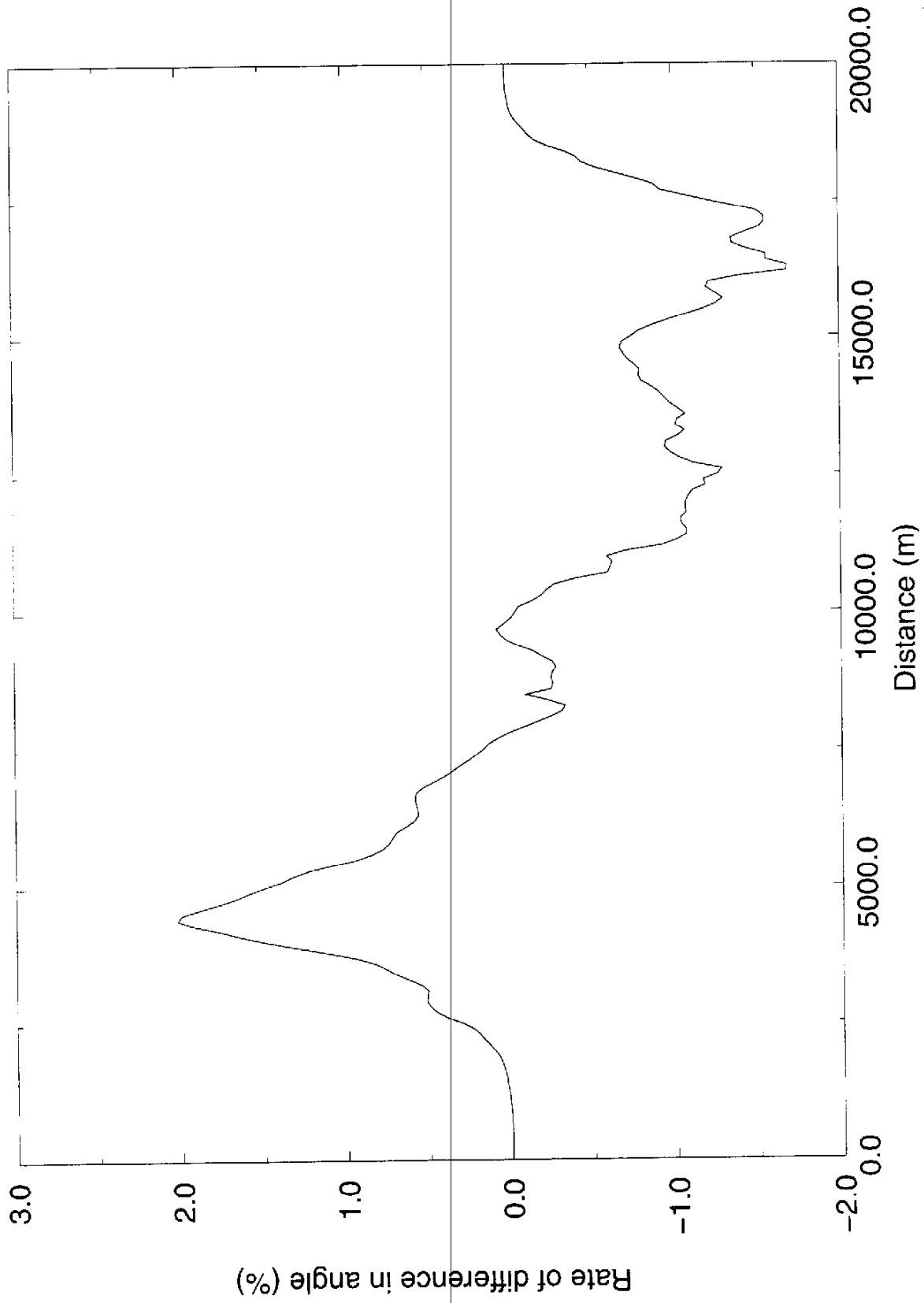


Fig. 28(b) Percent change in wave angle along reference line for same wave condition as Fig. 28(a).

with, C_g = the group celerity;
 α = the angle between the mean wave crest and the reference line;
and E = wave energy for each wave event.

And then, to develop a weighted average S_{xy} value for before and after dredging. Wave energy flux (C_g) is part of Eqn (16) so that S_{xy} would give a joint contribution from both wave energy and wave direction. This effort has been left for future research.

In summary, long term dredging alters the distribution of wave climate energy (and its direction) but not total energy along a distance that is 3-4 times the maximum lateral dimension of the borrow site. The percent energy change varies from zero to $\pm 10-15$ percent or more (maximum) over this distance. Is this maximum percentage change in wave climate energy significant? The next section is one way to answer this question and Question No. 8 in Section 4.1.

5.0 Decision Tool for Management

5.1 The Null-Hypothesis Theory

5.1.1 Difference Tests for Two Means. Each wave event of the 45,471 events for this study has in effect been transformed by the MIKE21.NSW model to produce a like number of wave “events” for each of 200 nodes along the 20,000m reference line. The total integrated wave energy is shown in Fig. 25. The integrated, total average wave energy over the 20,000m is

$$E_{\text{before}} = 226,596 \text{ kg-m/sec}^2$$

$$E_{\text{after}} = 226,011 \text{ kg-m/sec}^2$$

Average wave energy could be found for each nodal point and would also be on the order of 225,000 kg-m/sec². But as demonstrated in Fig. 29(a) before and Fig. 29 (b) after dredging, the distribution of wave energy is highly-skewed and not normally-distributed about the mean. This example is for $x = 10,000\text{m}$ and exactly in the middle of the reference line. It's clear that a large number of small wave energy events contribute to the major share of the total wave energy. The standard, null-hypothesis, statistical test for the significance of the difference of the means does not apply to the 45,471 wave data events. Instead, the difference test for two medians must be applied.

5.1.2 Difference Tests for Two Medians. The median test is designed to examine whether or not two (or more) samples came from populations having the same median. The median is the number such that 50 percent of the events are larger and 50 percent smaller. The median test for two populations can be found in any standard, statistical reference text (e.g., Conover, 1999)

In the analysis, the two data sets (here before and after dredging) are combined and the grand median (GM) determined which is the combined median. Then each data set is divided into data more than and less than the grand median. The frequency of events is arranged into a $2 * C$ contingency table where C is the total number of samples. It's assumed that:

1. each sample is random,
2. each sample is independent of all others,
3. the measurement scale is ordinal,
4. if all populations have the same median, they all have the same probability, P of an observation exceeding the grand median (GM),
5. The approximate null distribution is a chi-squared distribution.

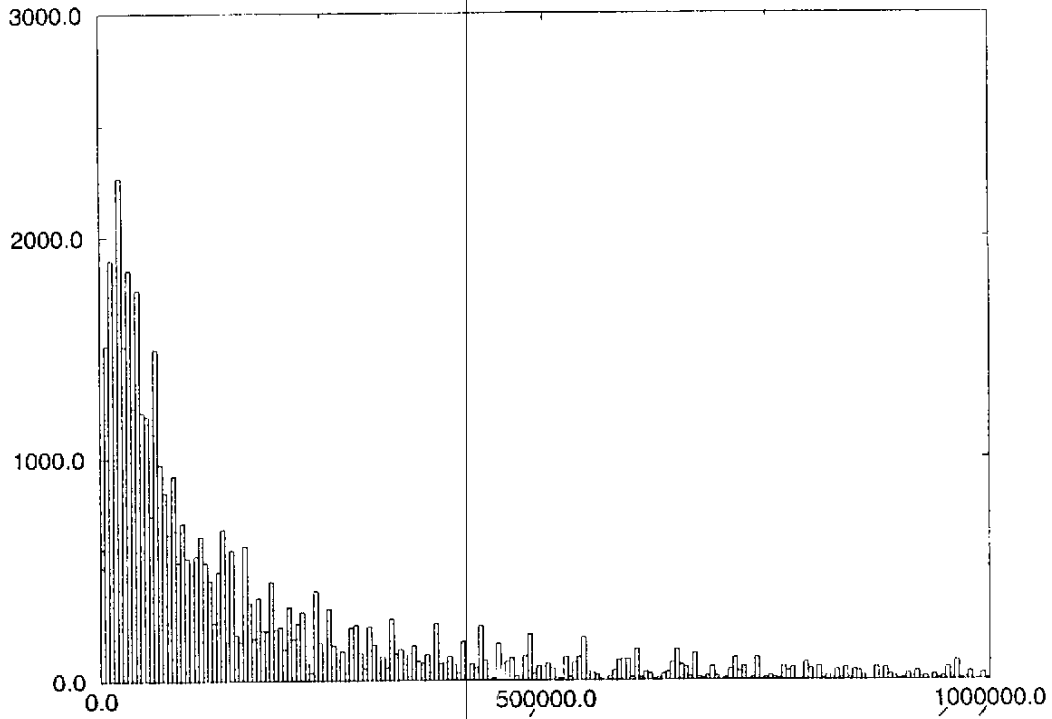


Fig. 29(a) Histogram of wave energy distribution at center of reference line showing highly skewed, non-Gaussian, wave energy distribution for 20 year wave climate. (Before dredging)

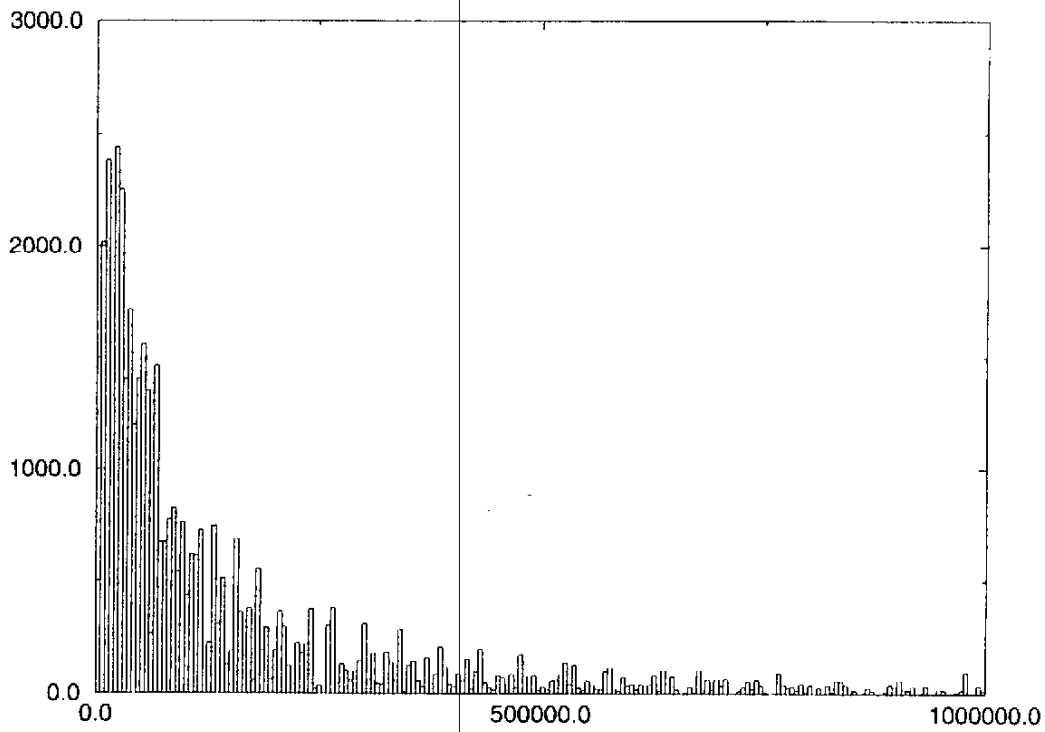


Fig. 29(b) Same as (a) above but after dredging the shoal.

A test statistic is computed (Conover, 1999, pg.218) for each population (before and after dredging) and a table consulted at the appropriate confidence level (95 percent) for either acceptance or rejection of the null-hypothesis.

5.2 Application to Sandbridge Shoal

For this study we have examined 22 positions along the reference line with all results summarized in Table V. As shown, some locations are (statistically speaking) from the same median population, hence the null-hypothesis is accepted, i.e. the wave energy climate after dredging remains unchanged. At other positions along the reference line, the null-hypothesis must be rejected signifying a statistically significant change in median wave energy after dredging. The percent change in total wave energy (see Fig. 26) is also listed in Table V for each nodal point considered. In general, wherever total wave energy change is greater than about ± 3 to 4%, the null-hypothesis is rejected, meaning that a change in total wave energy climate is statistically significant at the 95 percent confidence level. These zones are indicated in Fig. 30 using 4.0% as the cutoff percentage.

Table V

Nodal Point	Grand Median	Test Statistics	Null Hypothesis	Wave energy difference (%)
1	75896.2	0.0000	accept	0.0221
25	74176.8	0.0086	accept	1.129
33	62932.3	0.3723	accept	2.921
34	65605.6	10.1800	reject	3.358
50	76370.2	65.2510	reject	9.445
63	81091.1	4.0916	reject	3.940
64	82612.0	0.6654	accept	3.757
65	82663.8	3.5726	accept	3.670
75	80596.6	0.3178	accept	-1.579
76	82306.5	2.3876	accept	-2.312
77	83229.1	8.5510	reject	-3.837
100	82074.9	84.1280	reject	-16.896
118	80114.6	11.1180	reject	-7.004
119	81015.8	0.0370	accept	-5.519
120	81170.3	0.0022	accept	-4.681
121	80848.0	1.3687	accept	-4.210
125	83184.8	2.6190	accept	0.760
126	83020.7	12.8730	reject	2.692
127	81765.2	20.0400	reject	3.613
150	75613.7	10.6040	reject	4.685
179	60460.9	7.7560	reject	3.456
180	57289.1	3.5726	accept	2.89

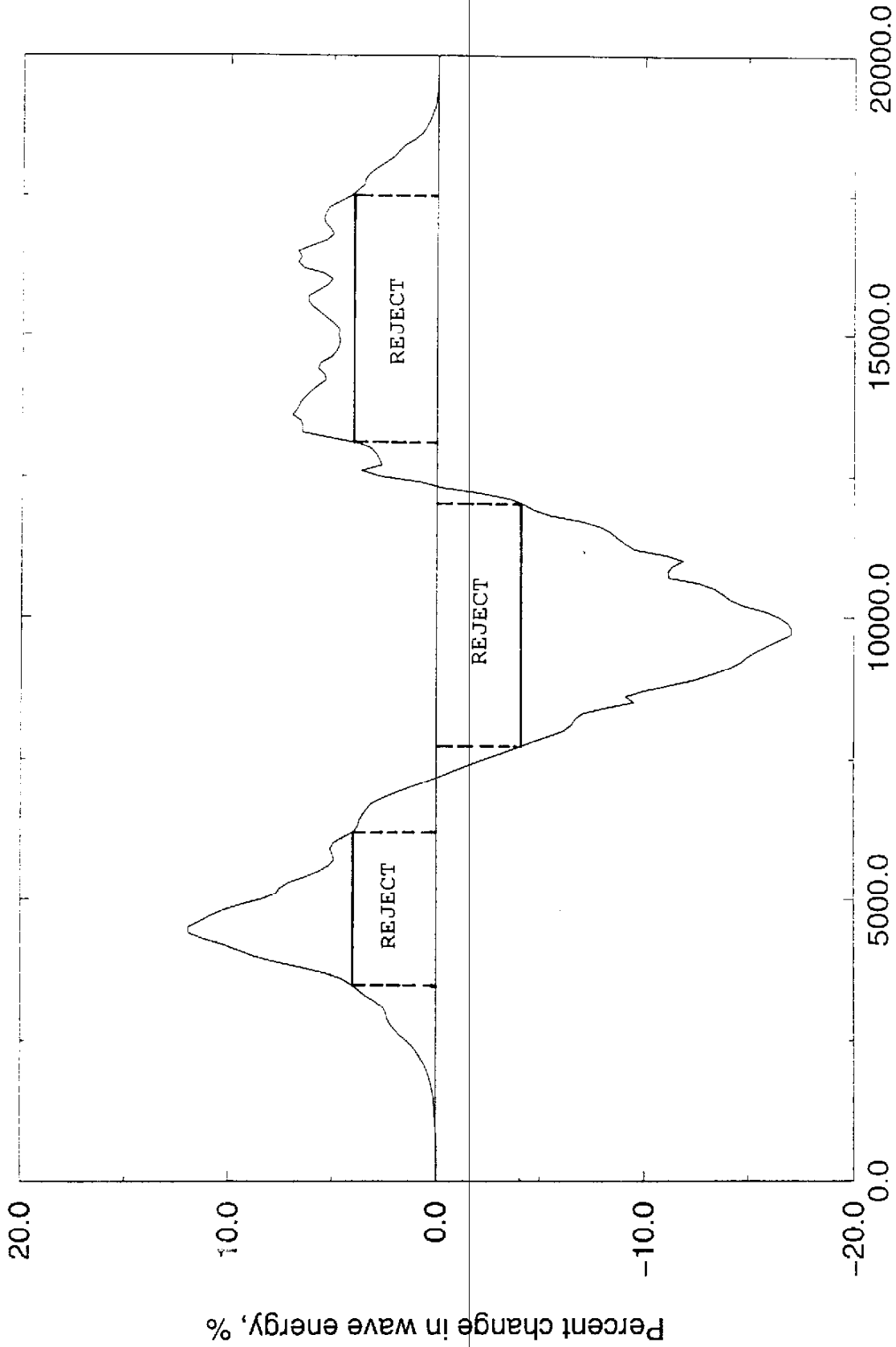


Fig. 30
 Percent change in total, wave climate energy showing regions of acceptance and rejection of the null-hypothesis using ≥ 4.0 percent as the cut-off value as found in this study.

The total length of the reference line with a significant total wave energy change is 12.6 km or 63.0 percent. Therefore, we conclude that since over 50 percent of the reference line experiences a wave climate modification, long-term dredging of sand from the Sandbridge Shoal will significantly alter the wave climate.

5.3 The Decision Tool Algorithm (DTA)

Computation of total wave climate energy along the reference line is facilitated by the algorithm given in Appendix B written in AWK Script. The median test computations and null-hypothesis test table could also be programmed so that combined, a Decision Tool Algorithm (DTA) can be developed to aid in management decisions for future permit applications. The length of the reference line that experiences wave climate alteration relative to the total length can become the criteria for rejection (or acceptance) of an offshore borrow site and the volume of sand removed. Alterations of the sand volume removed (area, depth, etc.) could influence the length of reference line affected. For this study, we assume that if 50 percent or more of the reference line length is significantly modified, then the site and long-term volume removed should be rejected.

The Minerals Management Service is ultimately responsible for setting the acceptance/rejection criteria as some percentage of the modified wave climate along the reference line. This study developed the methodology to provide the scientifically valid and statistically correct information for the MMS to set this criteria. The final decision for level of acceptance/rejection criteria is up to the MMS.

6.0 Generic Studies With Idealized Bathymetry

Boon and Hobbs (1998) looked at the nearshore Sandbridge, VA bathymetric profile represented by an equilibrium beach profile shape (Dean, 1997) with a mound rising 3m above the surface to represent the shoal. Lonza (1999) fitted the equilibrium beach profile shape to nearshore bathymetric charts at six locations (Atlantic City, NJ; Virginia Beach, VA; Ocracoke Island, NC; Naples, FL; and Galveston, TX) with 3-mile limit water depth ranging from 6 to 17m. Lonza (1999) then considered a dredged hole 3m deep, 2400m long and 1400m wide to represent the future dredging volume of about 10 million cubic meters. Each of these "generic studies" with an idealized, model bathymetry was intended to study how the complex wave model behaved in response to basic elements of bathymetry, i.e. the presence or absence of a shoal or dredged hole in its simplest configuration. These studies confirmed the basic response of waves to mounds and holes as illustrated in Figures 3 and 4, respectively.

These studies with idealized bathymetry, while informative cannot replace the study of the actual bathymetry, proposed borrow sites beyond the 3-mile limit, and proposed, long-term, sand volume removal demands at actual sites. For this purpose, the MMS issued RFP No. 1435-01-99-RP-3993 in March, 1999 for numerical wave model evaluations of 25 sand borrow sites in seven, East Coast state from New Jersey to Florida. The results reported herein should be useful to Applied Coastal Research and Engineering, Inc., Mashpee, MA who were awarded the contract.

7.0 Summary

7.1 Conclusions

Long-term dredging with significant sand removal from shoals and sand deposits in federal waters has the potential for negative impacts to the nearshore wave climate. In this study, we have employed the wave spectrum propagation model MIKE21.NSW to determine wave climate change landward of the Sandbridge Shoal borrow site in the Atlantic Ocean, in southeastern Virginia. And, we have considered a series of questions the answers of which will form the fundamental conclusions for this effort. As such, they become the methods to conduct the work for future sites.

1. Use the WIS hindcast information wave climate (Corps of Engineers, CERC) for 20 years at the site.
2. Use a spectral, wave transformation model for directional spectrums that includes shoaling, refraction, bottom friction, wave breaking and directional spreading transformation processes. Wave diffraction physics are not required in the model. The MIKE21.NSW model is a menu driven, user friendly model designed for improved productivity for multiple runs and is ideal for this application.
3. Calibrate the model coefficients (spreading index, bottom friction, wave breaking, etc.) using available wave data, wherever possible.
4. Use a reference line parallel to the shoreline to calculate wave heights and direction change rather than study the entire shadow zone landward of the borrow site.
5. Determine the water depth where at least 99 percent of all the waves break landward of this water depth. Make this depth contour the position of the reference line. Linear wave theory will then represent wave transformation processes for almost all the waves in the wave climate.
6. Analyze the wave climate information and reduce the data set to a useful number of wave direction bands (7-9) to condense the wave climate data set. The software program WHEREWAV as developed by CERC is useful for this purpose. Usually, 49 combination direction/period bands is sufficient.
7. Use a unit wave height (1.0m) to represent all the waves for each direction/period combination.
8. Run the model for each direction/period band and unit height at the boundary to calculate wave height multiplier coefficients along the reference line. Repeat for all direction/period

- band combinations and store the wave height multiplier coefficients along the reference line for each combination.
9. Calculate the wave energy density, the wave length, L and hence the wave energy for each wave event along the reference line. Use linear wave theory to find L.
 10. Determine the total, weighted energy in the wave climate by weighing all wave height events relative to the total number of waves in the wave climate.
 11. Use Corps of Engineers, District Office design memorandum, state and local city reports and other federal government and private beach nourishment needs to estimate the 25 and 50 year sand volume requirements for the borrow site. Determine the probable maximum sand volume needs from the borrow site for the selected design life.
 12. Modify the bathymetry for this volume removal from the site. Dredging depths are nominally 3 to 6 meters beyond the existing bathymetry.
 13. Repeat the above computation of total, weighted wave energy along the reference line for the after dredging bathymetry.
 14. Determine if the wave energy change (and wave direction change) is zero at both ends of the reference line. If not, extend the length of the reference line until no change is seen in the computed results.
 15. Calculate the percent wave energy change along the reference line.
 16. Use the Median Test (e.g. Conover, 1999) to test the null-hypothesis and significance of the difference of two medians at the 95 percent confidence level for about 10 locations along the reference line.
 17. Correlate with percent wave energy change and determine the relative length of the total reference line that rejects the null-hypothesis, i.e. will experience a statistically significant alteration of the wave climate.
 18. Reject the borrow site selected, or the total volume of sand removed and/or dredging plan (area, depth, etc.) if more that 50* percent of the reference line is impacted negatively.
 19. Modify the borrow site location, total sand volume removed, and/or dredging plan to reduce the length of reference line negatively impacted to less than 50* percent.
 20. Repeat the process until location, volume and/or dredging plan meets the MMS

* or the cut-off criteria established by the MMS

management criteria

In summary, we conclude that a clearly defined and rational methodology has been developed to quantify the before and after change in wave energy climate resulting from long-term sand dredging in federal waters. And, that environmental assessment criteria has been established for use by the MMS to make lease decisions that avoid negative impacts to the nearshore, water wave climate.

Applying the methodology and criteria to the long-term volume removal needs at the Sandbridge Shoal, we conclude that the wave climate will be negatively impacted. The total sand volume removed and/or dredging plan should be modified and re-analyzed by this method to determine the level of sand volume that meets the MMS management criteria.

7.2 Recommendations

The above method of analysis and criteria for management does not take into account wave direction change created by the borrow site. Further research is needed to quantify the composite, wave climate direction change along the reference line for all wave events. The radiation stress, longshore component, S_{xy} is one indicator that could be employed for it combines both wave energy and wave direction in the climate.

The gradient of S_{xy} drives the time-averaged, longshore current resulting from waves breaking at an angle along the shoreline. Together with breaking wave turbulence to lift sediment, the longshore current produces sediment transport along the coast. The net sediment transport direction is the resultant of all wave events in the climate. The change in wave direction along the reference line may alter the net sediment transport direction along the coast. Ultimately, changes in net sediment transport quantities and direction will produce changes in shoreline position (erosion and accretion) along the coast. The cut-off criteria* for acceptance and /or rejection of a borrow site could ultimately be established by its affect on long-term shoreline position.

We also recommend that the correlation between percent wave energy change and rejection by the null-hypothesis, median test be studied further at other sites. The methodology developed in this research effort is recommended for application at all the future borrow sites needing lease decisions by the MMS.

*Set at 50 percent of the reference line negatively impacted.

References

- Basco, D.R. and C.-S. Shin (1996) "Calibration of a Parametric, Wave Spectral Transformation Model in Chesapeake Bay", Final Rept., The Coastal Engineering Centre, Old Dominion Univ., Norfolk, Va. 40p
- Basco, D.R. (1998) "Beach Monitoring for Dam Neck-Year One", For NAVFAC, Norfolk, VA.
- Basco, D.R. and F.R. Lonza (1998) "Nearshore Wave Transformation Altered by Sand Volumes Removed from Borrow Areas for Beach Nourishment", Proceedings, WAVES' 97, vol. 1, ASCE, NY, pp.37-48
- Battjes, J.A. and J.P.F.M. Janssen(1978) "Energy Loss and Set-Up due Breaking of Random Waves", Proceedings, 16th ICCE. (Hamburg), ASCE, NY., pp 569-587
- Berkhoff, J.C.W. (1972) "Computation of Combined Refraction-Diffraction", Proceedings, 13th ICCE, ASCE, NY., vol.1 pp.471-490.
- Berkhoff, J.C.W., N. Booij and A.C. Radder (1982) "Verification of Numerical Wave Propagation Models for Simple Harmonic Linear Water Waves", Coastal Engineering, vol.6., pp225-279
- Bondzie, C. (1992) "Performance of Coastal Wave Models", M.Sc. Thesis, C.E. Dept., U of Maine, Orono, ME
- Bondzie, C. and B.G. Panchang (1993) "Effect of Bathymetric Complexities and Wind Generation in a Coastal Wave Propagation Model", Coastal Engineering, vol. 21, pp 333-366.
- Booij, N. (1985) "A Numerical Model for Wave Boundary Conditions in Port Design", Proceedings, Int'l. Conf. On Num. And Hyd. Modeling in Port Design, England, April, pp263-268
- Booij, N., L.H. Holthuijsen and R.C. Ris, (1996) "The SWAN Wave Model for Shallow Water", Proceedings, 25th ICCE (Orlando), ASCE, NY, pp 668-676
- Boon, J.D. and C.H. Hobbs, III (1998) "Part 3: Nearshore Waves and Currents, Observations and Modeling" in Environmental Studies Relative to Potential Sand Mining in the Vicinity of the City of Virginia Beach, Virginia, Final Rept., VIMS, Gloucester Pt., VA, Jan.
- Brooks, R.M. and W.A. Brandon (1995) "Hindcast Wave Information for U.S. Atlantic Coast: Update 1976-1993 with Hurricanes", WIS Rept. 33, Waterways Experiment Station, Corps of Engineers, Vicksburg, June

- Combe, A.J. and C.W. Soileau (1987) "Behavior of Man-Made Beach and Dune", Proceedings, Coastal Sediments '87, A.S.C.E., pp.1232-1242
- Conover, W.J. (1999) Practical Nonparametric Statistics, John Wiley and Sons, Inc., N.Y.,584p.
- Corps of Engineers (1996) "Ocean City, Maryland and Vicinity Water Resources Feasibility Report I", Appendix A, Coastal Engineering Analysis, WES, CERC, Vicksburg, MS.
- COE (1998) "Construction Solicitation and Specifications" for Beach Erosion Control Project, Sandbridge, VA, Corps of Engineers, Norfolk, D.O., March
- Dalrymple, R.H. and J.T. Kirby (1991) "REF/DIF, Version 2.3", Documentation Manual, Rept. No. CACR 91-2, Civil Engineering Dept., University of Delaware, Newark, 19p.
- de Adel et al. (1990) "Wave Model Application in Wadden Sea Ara", Proceedings,22nd ICCE (Delft), A.S.C.E., N.Y., pp 530-543
- Dingeman et al. (1986) "Directional Nearshore Wave Propagation and Induced Currents", Proceedings, 20th ICCE (Taipei), A.S.C.E., N.Y., p 1-15
- Holthuijsen, L.H., N. Booji and T.H.C. Herbers (1989) "A Prediction Model for Stationary, Short-Crested Waves in Shallow Waters With Ambient Currents", Coastal Engineering, Vol, 13, No.1, Elsevier, DenHaag, p 23-54
- Holthuijsen, L.H., et al. (1997) "A Verification of the Third-Generation Wave Model SWAN Along the Southern North Sea Coast, Proceedings, WAVES '97, Vol I A.S.C.E., N.Y., pp 49-63
- Komar, P.D. (1998) Beach Processes and Sedimentation, Prentice-Hall, N.Y., 2nd Edition, 544 p
- Komen, G.J., L. Caraleri, M. Donelan, K. Hasselmann, S. Hasselmann, and P.A.E.M. Janssen (1994) Dynamics and Modeling of Ocean Waves, Cambridge University Press, UK, 532 p
- Kimball, S.M. and J.K. Dame (1989) "Geotechnical Evaluation of Sand Resources on the Inner Shelf of Southern Virginia", Final Report, Virginia Institute of Marine Science, August
- List, J. (1996) personal communication
- Lonza, F.W. (1999) "The Effects of Offshore Mining of Beach Quality Sediments on Nearshore Wave Climate", unpublished M.S. thesis, Old Dominion University, Norfolk, VA

- Maa, J.P.-Y. and C.H. Hobbs, (1998) Physical Impact of Waves on Adjacent Coasts Resulting from Dredging at Sandbridge Shoal, Virginia, JCR.Vol.14(2), p 525-536
- Motyka, J.M. and D.H. Willis (1974) "The Effects of Refraction Over Dredged Holes", Proceedings, 14th ICCE (Copenhagen), A.S.C.E., N.Y.
- Ris, R.C., L.H. Holthuijsen and N.Booij (1994) :A Spectral Model for Waves in the Nearshore Zone", Proceedings, 24th, ICCE (Kobe), A.S.C.E., N.Y., pp 68-77
- Shore Protection Manual (1984), U.S. Gov't Printing Office, Washington, D.C.
- Swean, J. (1998a) :Beach Erosion Control and Hurricane Protection Project, Sandbridge Beach, Virginia Beach, VA", Construction Solicitation and Specifications, Norfolk D.O., Corps of Engineers, March (IFB No. DACW 65-98-B-0005)
- Swean, J. (1998b) "Beach Erosion Control and Hurricane Protection Project, Sandbridge Beach, Virginia Beach, VA", Plans, Norfolk D.O., Corps of Engineers, March
- Tolman, H.L. (1990) "Wind Wave Propagation in Tidal Seas", Ph.D. Dissertation, Delft University of Technology , Delft, The Netherlands, 135p
- Tolman, H.L.(1991) "Effects of Tides and Storm Surges on North Sea Wind Waves", J. Phys., Oceanography, Vol. 21, pp 766-781
- Trindade, et al. (1993) "Modeling Wave Penetration in Botany Bay", Proceedings, 11th Australian Conference on Coastal Engineering, Brisbane, Aug., pp 65-70
- VIMS (1996) "Fine-Grid Bathymetric Data", Virginia Institute of Marine Science, Gloucester Pt., VA
- Whitham, G.B. (1974) Linear and Nonlinear Waves, John Wiley and Sons, NY, 636p

Appendix A
WHEREWAV Results
for
WIS 2053, 20 yrs, 1976-1995

Virginia Beach, VA WHEREWAV Results

WAVE CLASSIFICATION & STATISTICS FOR INPUT TIME SERIES: Au2058
 THE FOLLOWING CLASSIFICATIONS ARE BASED ON A SHORELINE ORIENTATION OF:
 343.00

NUMBER OF RECORDS PROCESSED.....	58440
NUMBER OF CALM PRIMARY COMPONENT EVENTS	5
NUMBER OF CALM SECONDARY COMPONENT EVENTS	21532
NUMBER OF OFFSHORE TRAVELING PRIMARY COMPONENT EVENTS	10515
NUMBER OF OFFSHORE TRAVELING SECONDARY COMPONENT EVENTS	14329

DEFINITION OF ANGLE BANDS

ANGLE BAND NUMBER	RANGE WITH RESPECT TO NORTH	RANGE WITH RESPECT TO SHORE-NORMAL
1	343.00 : 348.75	90.00 : 84.25
2	348.75 : 11.25	84.25 : 61.75
3	11.25 : 33.75	61.75 : 39.25
4	33.75 : 56.25	39.25 : 16.75
5	56.25 : 78.75	16.75 : -5.75
6	78.75 : 101.25	-5.75 : -28.25
7	101.25 : 123.75	-28.25 : -50.75
8	123.75 : 146.25	-50.75 : -73.25
9	146.25 : 163.00	-73.25 : -90.00

DEFINITION OF PERIOD BANDS

PERIOD BAND NO.	RANGE OF WAVE PERIODS
1	0.0 < T < 5.0
2	5.0 < T < 7.0
3	7.0 < T < 9.0
4	9.0 < T < 11.0
5	11.0 < T < 13.0
6	13.0 < T < 15.0
7	15.0 < T < 17.0
8	17.0 < T < 23.0
9	23.0 < T

CLASSIFICATION OF COMBINED WAVE EVENTS BY ANGLE BAND

ANGLE BAND NUMBER	NUMBER OF EVENTS	AVERAGE WAVE ANGLE (W.R.T. SHORE-NORMAL)	AVERAGE WAVE HEIGHT	PERIOD BANDS
1	535	87.00	0.99	1 2 3
2	4255	73.26	1.01	1 2 3 4 5 6
3	3057	50.00	0.98	1 2 3 4 5
4	3186	27.57	0.92	1 2 3 4 5 6
5	8531	2.59	1.03	1 2 3 4 5 6 7 8
6	26837	-13.83	0.99	1 2 3 4 5 6 7 8 9
7	17359	-38.86	0.72	1 2 3 4 5 6 7 8 9
8	5272	-59.81	0.68	1 2 3 4 5 6
9	1467	-81.18	0.82	1 2 3 5

Virginia Beach, VA (continued)

CLASSIFICATION OF COMBINED WAVE EVENTS BY PERIOD BAND

PERIOD BAND NUMBER	NUMBER OF EVENTS	AVERAGE PERIOD	AVERAGE WAVE HEIGHT	ANGLE BANDS
1	9399	3.64	0.56	1 2 3 4 5 6 7 8 9
2	9878	5.44	1.06	1 2 3 4 5 6 7 8 9
3	15054	7.58	0.77	1 2 3 4 5 6 7 8 9
4	16428	9.46	0.83	2 3 4 5 6 7 8
5	10601	11.43	1.00	2 3 4 5 6 7 8 9
6	5931	13.39	1.20	2 4 5 6 7 8
7	2269	15.37	1.31	5 6 7
8	930	18.06	1.63	5 6 7
9	9	24.00	0.71	6 7

CLASSIFICATION OF PRIMARY WAVE EVENTS BY ANGLE BAND

ANGLE BAND NUMBER	NUMBER OF EVENTS	AVERAGE (W.R.T.)	WAVE ANGLE (SHORE-NORMAL)	AVERAGE WAVE HEIGHT	PERIOD BANDS
1	234		87.00	1.25	1 2 3
2	1786		73.64	1.23	1 2 3 5
3	1244		49.91	1.21	1 2 3 4 5
4	1384		27.63	1.34	1 2 3 4 5 6
5	5733		1.36	1.22	1 2 3 4 5 6 7 8
6	21636		13.74	1.11	1 2 3 4 5 6 7 8 9
7	12707		38.69	0.81	1 2 3 4 5 6 7 8 9
8	2650		58.84	0.87	1 2 3 4 5 6
9	546		81.48	1.18	1 2 3 5

CLASSIFICATION OF PRIMARY WAVE EVENTS BY PERIOD BAND

PERIOD BAND NUMBER	NUMBER OF EVENTS	AVERAGE PERIOD	AVERAGE WAVE HEIGHT	ANGLE BANDS
1	2698	3.83	0.72	1 2 3 4 5 6 7 8 9
2	5872	5.45	1.17	1 2 3 4 5 6 7 8 9
3	10172	7.59	0.87	1 2 3 4 5 6 7 8 9
4	12566	9.47	0.93	3 4 5 6 7 8
5	8716	11.45	1.11	2 3 4 5 6 7 8 9
6	5162	13.39	1.31	4 5 6 7 8
7	1920	15.37	1.46	5 6 7
8	805	18.08	1.82	5 6 7
9	9	24.00	0.71	6 7

Virginia Beach, VA (continued)

CLASSIFICATION OF SECONDARY WAVE EVENTS BY ANGLE BAND

ANGLE BAND NUMBER	NUMBER OF EVENTS	AVERAGE WAVE ANGLE (W.R.T. SHORE-NORMAL)	AVERAGE WAVE HEIGHT	PERIOD BANDS																
				1	2	3	4	5	6	7	8	9								
1	301	87.00	0.80																	
2	2469	72.99	0.85	1	2	3	4	5	6											
3	1813	50.06	0.82	1	2	3	4	5												
4	1802	27.53	0.60	1	2	3	4	5	6											
5	2798	5.12	0.64	1	2	3	4	5	6	7	8									
6	5201	-14.22	0.51	1	2	3	4	5	6	7	8									
7	4652	-39.34	0.46	1	2	3	4	5	6	7	8									
8	2622	-60.78	0.47	1	2	3	4	5												
9	921	-81.00	0.60	1	2	3														

CLASSIFICATION OF SECONDARY WAVE EVENTS BY PERIOD BAND

PERIOD BAND NUMBER	NUMBER OF EVENTS	AVERAGE PERIOD	AVERAGE WAVE HEIGHT	ANGLE BANDS																
				1	2	3	4	5	6	7	8	9								
1	6701	3.56	0.49	1	2	3	4	5	6	7	8	9								
2	4006	5.43	0.91	1	2	3	4	5	6	7	8	9								
3	4882	7.55	0.58	1	2	3	4	5	6	7	8	9								
4	3862	9.43	0.52	2	3	4	5	6	7	8										
5	1885	11.37	0.49	2	3	4	5	6	7	8										
6	769	13.39	0.47				2	5	6	7										
7	349	15.39	0.49								6									
8	125	17.96	0.43								6	7								
9	0	-	-																	

Appendix B

Software
Source Codes

```

#!/usr/local/bin/bash
#####
###
###      Shell script for calculating wave energy      ###
###
###                               Feb 1999            ###
###                               Takashi Okamoto     ###
###
#####
#
#   Setting pathes
#
wis=/home/okamoto/mms/data/WISdata
mik=/home/okamoto/mms/data/MIKEdata/expand/morextnt/refline
out=/home/okamoto/mms/script/long2
#gawk 'END{print NR}' $wis/tmp/wt* > $wis/tmp/number.data
#####
#
#   Calculating wave energy in each direction & period (refer to energy.awk)
#
time=1
dirc=1
while [ $time -le 7 ]
do
    dirc=1
    while [ $dirc -le 7 ]
    do
        gawk -f energy.awk -v avh="$wis"/tmp/wt"$time"d"$dirc".data
"$mik"/bfd"$dirc"t"$time".data >> "$out"/rsltbefor.data
        gawk -f energy.awk -v avh="$wis"/tmp/wt"$time"d"$dirc".data
"$mik"/afd"$dirc"t"$time".data >> "$out"/rsltafter.data
        let dirc=dirc+1
    done
    let time=time+1
done
#####
#
#   Adding up each component
#
gawk 'BEGIN{FS = "\n";RS=" \n"}
{for(i=1;i<=NF;i++){wh[i]=wh[i]+$i}}
END{for(i=1;i<=NF;i++){print wh[i]}}', "$out"/rsltbefor.data > "$out"/rb
gawk 'BEGIN{FS = "\n";RS=" \n"}
{for(i=1;i<=NF;i++){wh[i]=wh[i]+$i}}
END{for(i=1;i<=NF;i++){print wh[i]}}', "$out"/rsltafter.data > "$out"/ra
#####
#
#   Calculating the rate of change
#
gawk -f ratech.awk n=1 "$out"/rb n=2 "$out"/ra > "$out"/result

```



```

#####
###      Awk Script for calculating wave energy      ###
###                                          Feb 1999      ###
###                                          Takashi Okamoto  ###
###                                          #####
#
# Calculate wave length
#
BEGIN{
  getline < "/home/okamoto/mms/data/WISdata/tmp/number.data"
  number=$1
  pi=3.14159265
  d=6.5
  i=1
  while ( ( getline < avh ) > 0 ) {
    wavh[i]=$1
    timp[i]=$2
    l=100
    for ( count=1; count<=10; count++)
      {
        cosh=(exp(2*pi*d/l)+exp(-2*pi*d/l))/2
        sinh=(exp(2*pi*d/l)-exp(-2*pi*d/l))/2
        tanh=sinh/cosh
        f=1-9.8*($2^2)/2/pi*tanh
        df=1+9.8*($2^2)*d/(l^2)*(cosh^2-sinh^2)/(cosh^2)
        l=1-f/df
      }
    leng[i]=l
    i++
  }
  j=1
  #####
  ##### Calculate wave energy
  #####
  {
    for ( wr=1; wr<=i;wr++ )
      {
        ene[j]=ene[j]+1025*9.81*(wavh[wr]*$1)^2/8/number*leng[wr]
      }
    print ene[j]
    j++
  }
  #####
  END{ print " " }
}

```